

# Electronic States of Heavily Doped Molecular Crystals—Naphthalene. I. Theoretical

Hwei-Kwan Hong, and G. Wilse Robinson

Citation: *The Journal of Chemical Physics* **52**, 825 (1970);

View online: <https://doi.org/10.1063/1.1673062>

View Table of Contents: <http://aip.scitation.org/toc/jcp/52/2>

Published by the *American Institute of Physics*

---

---



## Electronic States of Heavily Doped Molecular Crystals—Naphthalene. I. Theoretical\*

HWEI-KWAN HONG AND G. WILSE ROBINSON

Arthur A. Noyes Laboratory of Chemical Physics,† California Institute of Technology, Pasadena, California 91109

(Received 1 August 1969)

The energy spectrum of heavily doped molecular crystals was treated in the Green's function formulation. The mixed-crystal Green's function was obtained by averaging over all possible impurity distributions. The resulting Green's function, which takes the form of an infinite perturbation expansion, was further approximated by a closed form suitable for numerical calculations. The density-of-states functions and optical spectra for binary mixtures of normal naphthalene and deuterated naphthalene were calculated using the pure-crystal density-of-states functions. The results showed that when the trap depth is large two separate energy bands persist, but when the trap depth is small only a single band exists. Furthermore, in the former case it was found that the intensities of the outer Davydov bands are enhanced whereas the inner bands are weakened. Comparisons with previous theoretical calculations and experimental results are also made.

## I. INTRODUCTION

The quantum states of solids are characterized by energy bands. The periodicity of the lattice requires the stationary-state wavefunctions to transform like the representations of the translational group, each associated with the reduced vector  $\mathbf{k}$ . Solid-state phenomena such as excitons,<sup>1,2</sup> phonons,<sup>3</sup> and magnons<sup>4</sup> are conveniently described within this group theoretical framework. In each case, the quasimomentum  $\hbar\mathbf{k}$  is always a good quantum number and is suitable for the description of energy systematics. On the other hand, many important physical systems, such as doped molecular crystals, alloys, copolymers, and some important biological macromolecules do not possess translational symmetry. The studies of their physical properties are usually hindered by the lack of symmetry. However, when the system does not deviate too much from a periodic system, theoretical analysis can usually be carried out by setting up the stationary-state wavefunctions for the periodic system and, then, allowing them to mix when the imperfection is introduced. One of the simplest systems for which this perturbation technique can be utilized is the system of isotopically mixed molecular crystals.

In the discussion of mixed molecular crystals, two different cases can be distinguished: (a) infinitely dilute mixed crystals and (b) heavily doped mixed crystals. Case (a) has been studied extensively during

the last decade both in theory and experiment. Experiments have been performed to study exciton trapping,<sup>5,6</sup> exciton migration,<sup>7</sup> and, more fundamentally, the intermolecular interactions that are responsible for the entire exciton band structure.<sup>8</sup> Considerable theoretical work,<sup>9–19</sup> mostly based on Koster and Slater's<sup>20–22</sup> formulation, was also carried out. This study was facilitated by the fact that, at very low concentrations of impurities, guest-guest interactions can be neglected. In the absence of such interactions, the exact site occupied by the impurity need not be specified and thus the disorder is actually minimized in this case.

For Case (b), the designation of guest and host is no longer very meaningful. Interactions between like molecules must now be taken into account. The situation is further complicated by the fact that the Hamiltonian of the system is only defined in an average sense. The ordering of the guests (or conversely, the ordering of the hosts) affects the energy spectrum of the system. A complete analysis would have to involve a statistical averaging of all the possible configurations.

Previous work on Case (b) is rather limited compared

\* G. C. Nieman and G. W. Robinson, J. Chem. Phys. **39**, 1298 (1963).

† M. A. El-Sayed, M. T. Wauk, and G. W. Robinson, Mol. Phys. **5**, 205 (1962).

‡ S. D. Colson and G. W. Robinson, J. Chem. Phys. **48**, 2550 (1968).

§ D. M. Hanson, R. Kopelman, and G. W. Robinson, J. Chem. Phys. **51**, 212 (1969).

|| E. I. Rashba, Opt. Spektrosk. **2**, 568 (1957).

¶ E. I. Rashba, Fiz. Tverd. Tela **4**, 3301 (1962) [Sov. Phys.—Solid State **4**, 2417 (1963)].

‡ R. G. Body and I. G. Ross, Australian J. Chem. **19**, 1 (1966).

§ S. Takeno, J. Chem. Phys. **44**, 853 (1966).

|| D. P. Craig and M. R. Philpott, Proc. Roy. Soc. (London) **A290**, 583 (1966).

¶ D. P. Craig and M. R. Philpott, Proc. Roy. Soc. (London) **A290**, 602 (1966).

‡ D. P. Craig and M. R. Philpott, Proc. Roy. Soc. (London) **A293**, 213 (1966).

§ B. S. Sommer and J. Jortner, J. Chem. Phys. **50**, 187 (1969).

¶ B. S. Sommer and J. Jortner, J. Chem. Phys. **50**, 822 (1969).

|| I. M. Lifschitz, Advan. Phys. **13**, 483 (1964).

‡ Y. A. Izyumov, Advan. Phys. **14**, 569 (1965).

§ G. F. Koster and J. C. Slater, Phys. Rev. **95**, 1167 (1954).

¶ G. F. Koster and J. C. Slater, Phys. Rev. **96**, 1208 (1954).

‡ G. F. Koster, Phys. Rev. **95**, 1436 (1954).

\* This work was supported in part by the U.S. Army Research Office—Durham, Contract No. DA-31-124-ARO-D-370.

† Contribution No. 3914.

‡ (a) J. Frenkel, Phys. Rev. **37**, 17, 1276 (1931); (b) A. S. Davydov, *Theory of Molecular Excitons* (McGraw-Hill Book Co., New York, 1962); (c) A. S. Davydov, Usp. Fiz. Nauk **82**, 393 (1964) [Sov. Phys.—Usp. **7**, 145 (1964)].

§ (a) D. P. Craig and S. H. Walmsley, *Physics and Chemistry of the Organic Solid State*, D. Fox, M. M. Labes, and A. Weissberger, Eds. (Interscience Publishers, Inc., New York, 1963), Vol. 1, Chap. 10; (b) S. A. Rice and J. Jortner, *Physics and Chemistry of the Organic Solid State*, D. Fox, M. M. Labes, and A. Weissberger, Eds. (Interscience Publishers, Inc., New York, 1967), Vol. 3, Chap. 4.

¶ C. Kittel, *Quantum Theory of Solids* (John Wiley & Sons, Inc., New York, 1963).

‡ *Excitons, Magnons and Phonons*, A. B. Zahlan, Ed. (Cambridge University Press, London, 1968).

with Case (a). Broude and Rashba's method,<sup>23</sup> which is based on the assumption that like molecules at like sites have the same excitation amplitude, is expected to be useful only for equimolecular admixtures. Craig and Philpott's<sup>13-15</sup> super-lattice method, while mathematically more manageable, is limited by the size of the supercell that can be handled. Since a finite number of molecules are treated, a finite number of states are obtained. In addition, only discrete compositions can be considered. In order to approach the true situation, the supercell has to be enormously large. The most serious drawback to the latter approach seems to rest with the basic assumption that impurities are arranged on a superlattice in translationally equivalent sets. This immediately leaves out all the aperiodic distributions in the averaging process. When attempts are made to remedy this situation, and bigger cells are chosen, the problem becomes computationally intractable. In actual numerical calculations, Craig and Philpott calculated only the  $\mathbf{k}=0$  component of the density of states for naphthalene- $h_8$  and  $d_8$ . They did not treat spectra involving shallower energy gaps.

The only experiments to date on concentrated mixed crystals have been those of Broude and Rashba<sup>23</sup> and Sheka<sup>24,25</sup> on benzenes and naphthalenes, respectively. Sheka's experiments were carried out at 22°K. The spectra obtained were rather broad and some of the fine structure caused by "cluster states" typically observed in the spectra of certain mixed crystals became obscure. Furthermore, in this work weighed samples with known concentrations were not used. Rather, Broude and Rashba's approximate formula was fit to the spectra in order to determine the concentrations. Thus, on the experimental side, additional work using weighed samples at lower temperatures seems desirable.

In Part I of this series, we consider the general formulation for isotopically mixed crystals with various compositions using the Green's function method. Exact expressions for the mixed-crystal Green's function are presented in terms of an infinite perturbation expansion. An approximate formula in closed form suitable for actual numerical calculations is also given and applied specifically to the mixed crystals of naphthalenes with different trap depths. Density-of-states functions and optical spectra for the mixed crystals were calculated using two different sets of pure-crystal density-of-states functions, one based on Craig and Walmsley's<sup>26</sup> octopole model and the other experimentally determined by Colson *et al.*<sup>27</sup> In Part II new experimental data on the absorption spectra and emission spectra at dif-

ferent temperatures will be analyzed and discussed in the light of the theoretical model.

The purpose of the present work is manifold: (a) As a prototype of disordered systems, heavily doped mixed crystals present a physically amenable system for more or less exact treatment. Understanding the electronic states of this system is the first step toward the understanding of more complicated disordered systems. (b) A unified theory connecting the electronic states and optical properties of pure crystals on the one hand and infinitely dilute mixed crystals on the other is long overdue. The present investigation will in many ways help fill the gap. (c) Heavily doped mixed crystals provide additional detailed information concerning the guest-guest interactions in molecular crystals. An exact theoretical analysis of this system not only provides a check on the gross density-of-states function but also allows the individual pairwise interactions to be determined. (d) These studies also provide answers to the question of whether Davydov splitting is primarily due to symmetry relations or resonance coupling, as raised frequently by some of the workers in this field.<sup>2b 16</sup>

Among the general theories of disordered solids, the multiple-scattering formulation of Lax<sup>28</sup> has been the most successful. This pioneering work was followed by the elegant mathematical analysis of Yonezawa and Matsubara<sup>29</sup> (YM). The present theoretical development parallels closely YM's work except that their theory is generalized to the case of multiple-branched exciton bands and particularized to the problem of isotopically mixed crystals.

## II. THEORY

### A. Perturbation Method for Isotopically Mixed Crystals

The system under discussion consists of two types of molecules with different excitation energies. For dilute mixed crystals, it is common practice to denote the major component as the *host* and the minor component as the *guest*. However, in the case of heavily doped mixed crystals, the distinction between the host and the guest is not very meaningful. We will simply refer to them as the A component and the B component. We take the A component to have the higher excitation energy (e.g., naphthalene with a higher degree of deuteration).

We start with the total Hamiltonian of a pure crystal composed of A molecules

$$H^0 = \sum_i H_i^A + \sum_{i,j} \sum_{\alpha,\beta} V_{ij}^{\alpha\beta}, \quad (1)$$

where  $H_i^A$  is the Hamiltonian of an A molecule at site  $i$ , and  $V_{ij}^{\alpha\beta}$  is the interaction between an A molecule

<sup>23</sup> V. L. Broude and E. I. Rashba, *Fiz. Tverd. Tela* **3**, 1941 (1961) [*Sov. Phys.—Solid State* **3**, 1415 (1962)].

<sup>24</sup> E. F. Sheka, *Opt. Spektrosk.* **10**, 684 (1961) [*Opt. Spectrosc.* **10**, 360 (1961)].

<sup>25</sup> E. F. Sheka, *Bull. Acad. Sci. USSR Phys. Ser.* **27**, 501 (1963).

<sup>26</sup> D. P. Craig and S. H. Walmsley, *Mol. Phys.* **4**, 113 (1961).

<sup>27</sup> S. D. Colson, D. M. Hanson, R. Kopelman, and G. W. Robinson, *J. Chem. Phys.* **48**, 2215 (1968).

<sup>28</sup> M. Lax, *Rev. Mod. Phys.* **23**, 287 (1951); *Phys. Rev.* **85**, 621 (1952).

<sup>29</sup> (a) F. Yonezawa and T. Matsubara, *Progr. Theoret. Phys. (Kyoto)* **35**, 357 (1966); (b) **35**, 759 (1966); (c) **37**, 1346 (1967).

at site  $i$  and an A molecule at site  $j$ . When the B component is introduced as an impurity, the Hamiltonian becomes

$$H' = \sum_i H_i^A + \sum_p H_p^B + \sum_{i>j} V_{ij}^{AA} + \sum_{p>q} V_{pq}^{BB} + \sum_i \sum_p V_{ip}^{AB}, \quad (2)$$

where  $H_i^A$  is the Hamiltonian of an A molecule at site  $i$ ,  $H_p^B$  is the Hamiltonian of a B molecule at site  $p$ ,  $V_{ij}^{AA}$  is the interaction between an A molecule at site  $i$  and an A molecule at site  $j$ ,  $V_{pq}^{BB}$  is the interaction between a B molecule at site  $p$  and a B molecule at site  $q$ , and  $V_{ip}^{AB}$  is the interaction between an A molecule at site  $i$  and a B molecule at site  $p$ .

We limit our discussion to the case of isotopically mixed crystals. In this case, all the interactions between A and A, B and B, and A and B can be assumed to be equal; hence,

$$H' = \sum_i H_i^A + \sum_p H_p^B + \sum_{n>m} V_{nm}, \quad (3)$$

where  $V_{nm}$  is the interaction between molecules without making a distinction between A and B.

The mixed-crystal Hamiltonian can be expressed in terms of the pure-crystal Hamiltonian and a perturbation:

$$H' = H^0 + \sum_p t_p, \quad (4)$$

where  $t_p = H_p^B - H_p^A$  is the localized perturbation acting only on the  $p$ th site occupied by the B molecule. For isotopically mixed crystals, the  $t_p$ 's arise primarily from the change in nuclear kinetic energy as a result of isotopic substitution.

In the present discussion, the zero-zero band of an electronic transition is considered as an isolated Frenkel exciton band. It has been shown<sup>13</sup> that under the assumption of a localized perturbation, which is

implied in Eq. (4), the introduction of isotopic impurities does not cause the mixing between different excited states if initially they are constructed properly to include possible configurational interactions. The existence of vibrational sublevels in a particular electronic state also has little effect on the pure electronic transition. In the limit of weak coupling, the vibrational spacings are certainly larger than the exciton bandwidth. Within this limit it was pointed out by several authors<sup>13,16</sup> that the one-band approximation is very likely adequate for most purposes.

The eigenfunctions of the pure-crystal Hamiltonian can be constructed from site functions with Bloch symmetry<sup>30</sup>:

$$\Psi(\mathbf{k}) = \sum_i \exp(i\mathbf{k} \cdot \mathbf{R}_i) \Phi_i, \quad (5)$$

where

$$\Phi_i = \phi_i^* \prod_{j \neq i} \phi_j$$

is the wavefunction corresponding to the excitation localized at site  $i$ . There are as many such "site functions" as the number of molecules per unit cell. These site functions reduce the Hamiltonian matrix to small blocks characterized by their wave vectors. Further reduction within the block is not possible except in some special cases, for example, the  $\mathbf{k} = 0$  block. However, in the limit of short-range interactions such as those encountered in molecular crystals of benzene and naphthalene, Colson *et al.*<sup>30</sup> have shown that the factor-group operations can be applied to all the  $\mathbf{k}$  blocks, and simple linear combinations of site functions can be used for all the  $\mathbf{k}$  states. The approximation greatly simplifies the theoretical derivations, as will be seen later in Sec. II.C. Using this approximation for the lowest excited singlet state ( ${}^1B_{2u}$ ) of the naphthalene crystal (two molecules per unit cell) the two site functions are<sup>31</sup>

$$\begin{aligned} \Psi_{A_u}(\mathbf{k}) &= N^{-1/2} [\Psi_\alpha(\mathbf{k}) + \Psi_\beta(\mathbf{k})] = N^{-1/2} \left[ \sum_\alpha \exp(i\mathbf{k} \cdot \mathbf{R}_\alpha) |\alpha\rangle + \sum_\beta \exp(i\mathbf{k} \cdot \mathbf{R}_\beta) |\beta\rangle \right], \\ \Psi_{B_u}(\mathbf{k}) &= N^{-1/2} [\Psi_\alpha(\mathbf{k}) - \Psi_\beta(\mathbf{k})] = N^{-1/2} \left[ \sum_\alpha \exp(i\mathbf{k} \cdot \mathbf{R}_\alpha) |\alpha\rangle - \sum_\beta \exp(i\mathbf{k} \cdot \mathbf{R}_\beta) |\beta\rangle \right], \end{aligned} \quad (6)$$

where  $|\alpha\rangle$  is the wavefunction corresponding to the excitation at  $\alpha$  sites,  $|\beta\rangle$  is the wavefunction corresponding to the excitation at  $\beta$  sites, and the summation is carried over all the  $\alpha$  sites and all the  $\beta$  sites. The corresponding energies are found to be

$$\begin{aligned} E_{A_u}(\mathbf{k}) &= \epsilon_A + I_{\alpha\alpha}(\mathbf{k}) + I_{\alpha\beta}(\mathbf{k}), \\ E_{B_u}(\mathbf{k}) &= \epsilon_A + I_{\alpha\alpha}(\mathbf{k}) - I_{\alpha\beta}(\mathbf{k}), \end{aligned} \quad (7)$$

where  $I_{\alpha\alpha}$  and  $I_{\alpha\beta}$  are the modulated sums<sup>2a</sup> of translationally equivalent and inequivalent interactions,

respectively.  $\epsilon_A$  corresponds to the mean of the exciton band. It is also equal to the gas-phase transition energy minus the site shift that is caused by the static interactions between the molecule and its environment.

We now expand the mixed-crystal wavefunctions in terms of the complete set of pure-crystal wavefunctions:

$$\psi = \sum_{\mathbf{k}^+} f(\mathbf{k}^+) |\mathbf{k}^+\rangle + \sum_{\mathbf{k}^-} f(\mathbf{k}^-) |\mathbf{k}^-\rangle, \quad (8)$$

where  $|\mathbf{k}^+\rangle = \Psi_{A_u}(\mathbf{k})$  and  $|\mathbf{k}^-\rangle = \Psi_{B_u}(\mathbf{k})$ . For convenience we have put  $\mathbf{k} = \mathbf{k}^+$  for  $A_u$  states and  $\mathbf{k} = \mathbf{k}^-$

<sup>30</sup> S. D. Colson, R. Kopelman, and G. W. Robinson, J. Chem. Phys. **47**, 27 (1967).

<sup>31</sup> The molecular axes are assigned according to the same convention as in Ref. 27. The  $C_2$  interchange operation was used rather than the reflection operation cf. Ref. 26).

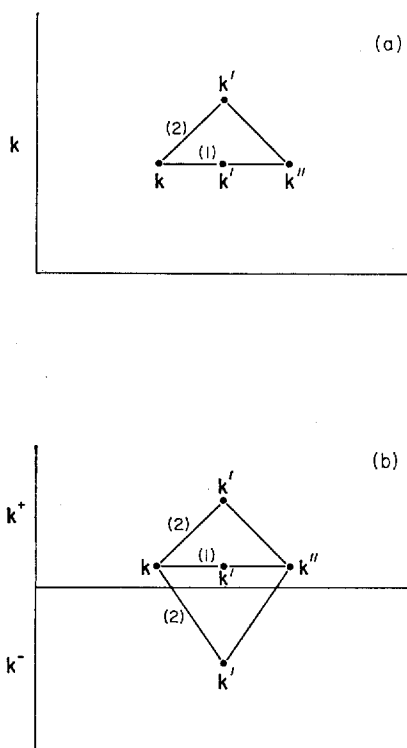


FIG. 1. Possible scattering routes contained in  $M_2$  for (a) single-branched exciton band and (b) double-branched exciton band. Route (1) corresponds to  $\delta(p_1)\delta(p_2)=1$ , and Route (2) corresponds to  $\delta(p_1+p_2)=1$ . The definition of the delta function used here is given in the text.

$B_u$  states. As a vector,  $\mathbf{k}^+$  may be equal to  $\mathbf{k}^-$  but  $|\mathbf{k}^+\rangle$  is uniquely different from  $|\mathbf{k}^-\rangle$ . The corresponding energies for the  $\mathbf{k}^+$  and  $\mathbf{k}^-$  states are

$$\begin{aligned} E_{\mathbf{k}^+} &= \epsilon_A + \epsilon(\mathbf{k}^+), \\ E_{\mathbf{k}^-} &= \epsilon_A + \epsilon(\mathbf{k}^-), \end{aligned} \quad (9)$$

with  $\epsilon(\mathbf{k}^+) = I_{\alpha\alpha} + I_{\alpha\beta}$  and  $\epsilon(\mathbf{k}^-) = I_{\alpha\alpha} - I_{\alpha\beta}$ .

In the derivation of secular equations, we note that  $t_p$  acts only on the nuclear part of the Born-Oppenheimer wavefunctions. The following expressions can be easily obtained:

$$\begin{aligned} \langle \Phi_i | t_p | \Phi_j \rangle &= 0 \quad \text{if } i \neq j, \\ \langle \Phi_i | t_p | \Phi_i \rangle &= (\Delta^* - \Delta^0) \delta_{ip} + \Delta^0, \\ \Delta^* &= \langle \chi^* | t | \chi^* \rangle, \\ \Delta^0 &= \langle \chi^0 | t | \chi^0 \rangle, \end{aligned} \quad (10)$$

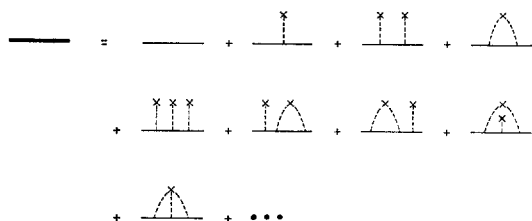


FIG. 2. Diagrams representing the expansion of the true propagator in terms of the free propagator.

where  $\chi^*$  and  $\chi^0$  are the nuclear wavefunctions for the excited and ground states, respectively, of the A molecule. We drop the site index because the expressions are independent of site.  $\Delta^*$  corresponds to the first-order value of the zero-point energy difference between A and B in the excited state, and  $\Delta^0$  corresponds to the same quantity at the ground state. Since the wavefunctions for A and B are expected to be very similar we can assume that the first-order correction is adequate and set  $\Delta^* - \Delta^0$  equal to  $E_B - E_A$ , i.e., the difference in excitation energies or simply the trap depth  $\Delta$ .

Notice that if the site shift does not depend on isotopic substitution, which is the case in naphthalene<sup>8</sup> but not in benzene,<sup>32</sup> we can set  $\Delta = \epsilon_B - \epsilon_A$ , where  $\epsilon_B$  is the mean of the exciton band for the B molecule.

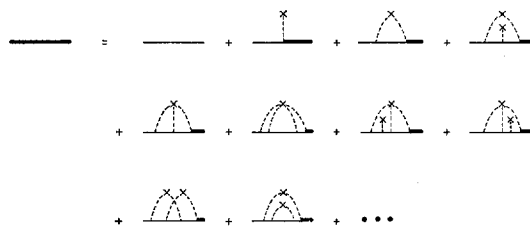


FIG. 3. Diagrams representing the expansion terms to be summed if the last propagator  $G_0$  in Fig. 2 is replaced by the true propagator  $[G]$ .

With the aid of Eq. (10), the secular equations are found to be

$$\begin{aligned} (E + N_B \Delta^0 - E_{\mathbf{k}^+}) f(\mathbf{k}^+) &= (\Delta/N) \\ &\times \left\{ \sum_{\mathbf{k}'^+} f(\mathbf{k}'^+) [\rho_\alpha(\mathbf{k}^+ - \mathbf{k}'^+) + \rho_\beta(\mathbf{k}^+ - \mathbf{k}'^+)] \right. \\ &\left. + \sum_{\mathbf{k}'^-} f(\mathbf{k}'^-) [\rho_\alpha(\mathbf{k}^+ - \mathbf{k}'^-) - \rho_\beta(\mathbf{k}^+ - \mathbf{k}'^-)] \right\}, \end{aligned} \quad (11a)$$

$$\begin{aligned} (E + N_B \Delta^0 - E_{\mathbf{k}^-}) f(\mathbf{k}^-) &= (\Delta/N) \\ &\times \left\{ \sum_{\mathbf{k}'^+} f(\mathbf{k}'^+) [\rho_\alpha(\mathbf{k}^- - \mathbf{k}'^+) - \rho_\beta(\mathbf{k}^- - \mathbf{k}'^+)] \right. \\ &\left. + \sum_{\mathbf{k}'^-} f(\mathbf{k}'^-) [\rho_\alpha(\mathbf{k}^- - \mathbf{k}'^-) + \rho_\beta(\mathbf{k}^- - \mathbf{k}'^-)] \right\}, \end{aligned} \quad (11b)$$

where

$$\begin{aligned} \rho_\alpha(\mathbf{k} - \mathbf{k}') &= \sum_{\alpha} \exp[-i(\mathbf{k} - \mathbf{k}') \cdot \mathbf{R}_\alpha], \\ \rho_\beta(\mathbf{k} - \mathbf{k}') &= \sum_{\beta} \exp[-i(\mathbf{k} - \mathbf{k}') \cdot \mathbf{R}_\beta], \end{aligned}$$

$N_B$  = total number of B molecules.

The summations  $\sum_{\alpha}$  and  $\sum_{\beta}$  are carried out over all  $\alpha$  sites and  $\beta$  sites occupied by the B molecules. If we use the mixed-crystal ground state as the energy zero,  $N_B \Delta^0$  terms can be dropped. The solutions of Eqs. (11) would correspond to the exact excitation energies in mixed crystals.

<sup>32</sup> S. D. Colson, J. Chem. Phys. 48, 3324 (1968).

Several features of the secular equations can be noted:

(1) The introduction of impurities not only causes the mixing among the  $\mathbf{k}^+$  states and the  $\mathbf{k}^-$  states, but it also causes the mixing between  $\mathbf{k}^+$  states and  $\mathbf{k}^-$  states. For a multiple-branched exciton band, the full interaction matrix must be used to calculate the perturbed energy states.

(2) It is apparent that for a single impurity molecule there is no need to specify whether the impurity occupies the  $\alpha$  or  $\beta$  site. However, when more than one

impurity is present, the energy states depend on the exact sites occupied by the impurities. This is manifested by the fact that the coupling matrix elements among all  $\mathbf{k}$  states depend on whether the impurities occupy  $\alpha$  or  $\beta$  sites.

We have derived the secular equations using a delocalized representation. For dilute mixed crystals, the corresponding equations can be converted to a localized set. This is essentially the method of Koster and Slater.<sup>20-22</sup> For example, the energy matrix for dimers is found to be

$$\left| \begin{array}{c} 1 - \frac{\Delta}{N} \sum_{\text{all } \mathbf{k}} \frac{1}{(E - E_{\mathbf{k}})} \\ - \frac{\Delta}{N} \left( \sum_{\mathbf{k}^+} \frac{\exp(-i\mathbf{k}^+ \cdot \mathbf{R})}{E - E_{\mathbf{k}^+}} \pm \sum_{\mathbf{k}^-} \frac{\exp(-i\mathbf{k}^- \cdot \mathbf{R})}{E - E_{\mathbf{k}^-}} \right) \end{array} \right| = 0.$$

The upper sign must be used for translationally equivalent dimers, and the lower sign must be used for translationally inequivalent dimers.  $\mathbf{R}$  is the distance between the impurities. Similar expressions were obtained by Craig and Philpott.<sup>14</sup>

In the next section we will use the secular equations (11a) and (11b) to derive the Green's function. By solving the Green's function we can calculate the density-of-states function and also the optical absorption spectrum for heavily doped mixed crystals.

## B. The Green's Function Method

A Green's function is conveniently defined by the operator equation

$$G = (E - H')^{-1}, \quad (12)$$

where  $H'$  is the Hamiltonian of the system. In terms of any complete orthonormal set  $\{\mathbf{k}\}$ , Eq. (12) can be written in a matrix representation:

$$\sum_{\mathbf{k}''} (E - H')_{\mathbf{k}\mathbf{k}''} G_{\mathbf{k}''\mathbf{k}'} = \delta_{\mathbf{k}\mathbf{k}'}. \quad (13a)$$

It follows immediately that

$$G_{\mathbf{k}\mathbf{k}'} = \sum_n [f_n^*(\mathbf{k}) f_n(\mathbf{k}') / (E - E_n)], \quad (13b)$$

where  $E_n$  is an eigenvalue of  $H'$ , and  $f_n(\mathbf{k})$  is the

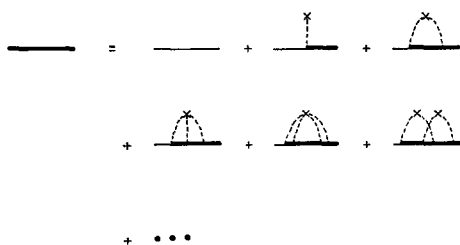


FIG. 4. Diagrams representing the expansion terms to be summed if all but the first propagator in Fig. 2 are replaced by the true propagator  $[G]$ .

expansion coefficient of the eigenstate  $|n\rangle$  onto the basis state  $|\mathbf{k}\rangle$ , or equivalently  $f_n(\mathbf{k}) = \langle \mathbf{k} | n \rangle$ .

Following Goodings and Mozer,<sup>33</sup> we define a weighted density-of-states function:

$$g_{\mathbf{k}\mathbf{k}'}(E) = \sum_n f_n^*(\mathbf{k}) f_n(\mathbf{k}') \delta(E - E_n). \quad (14)$$

Equation (13b) can then be written in an integral form,

$$G_{\mathbf{k}\mathbf{k}'}(E) = \int [g_{\mathbf{k}\mathbf{k}'}(E') dE' / (E - E')].$$

Using the symbolic identity ( $\epsilon \rightarrow 0^-$ )

$$(E + i\epsilon - E')^{-1} = P(E - E')^{-1} + i\pi \delta(E - E'),$$

the Green's function can be separated into a real part and an imaginary part:

$$\text{Re} G_{\mathbf{k}\mathbf{k}'}(E + i\epsilon) = P \int [g_{\mathbf{k}\mathbf{k}'}(E') dE' / (E - E')], \quad (15a)$$

$$\text{Im} G_{\mathbf{k}\mathbf{k}'}(E + i\epsilon) = \pi g_{\mathbf{k}\mathbf{k}'}(E). \quad (15b)$$

The energy states of the condensed system can be best described by a normalized density-of-states function  $D(E)$  defined as the fraction of states per unit energy or

$$D(E) = N^{-1} \sum_n \delta(E - E_n).$$

Through Eqs. (14) and (15),  $D(E)$  is related to the Green's function by the expression

$$D(E) = N^{-1} \text{Tr} g = (N\pi)^{-1} \text{Im Tr} G(E + i\epsilon). \quad (16)$$

If we identify the  $\{\mathbf{k}\}$  set as the delocalized basis set in Eq. (6), the familiar  $\mathbf{k} = 0$  selection rule implies that the transition probability to an eigenstate  $|n\rangle$  is equal to the square of its projection onto the  $\mathbf{k} = 0$  state times the square of the transition moment of the  $\mathbf{k} = 0$  state.

<sup>33</sup> D. A. Goodings and B. Mozer, Phys. Rev. **A136**, 1093 (1964).

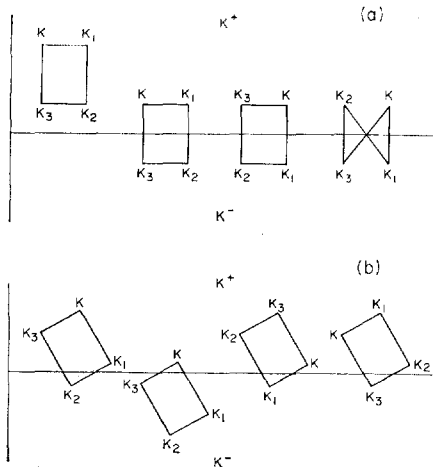


FIG. 5. Possible scattering routes given by  $\delta(k-k_1+k_2-k_3) \times \delta(k_1-k_2+k_3-k)$  according to our definition of the delta functions. Terms to be summed are those in (a) and terms *not* to be summed are those in (b).

Since two Davydov components exist, we define two optical absorption functions  $I_{A_u}(E)$  and  $I_{B_u}(E)$  as

$$I_{A_u}(E) = \sum_n f_n^*(\mathbf{k}^+ = \mathbf{0}) f_n(\mathbf{k}^+ = \mathbf{0}) \delta(E - E_n),$$

$$I_{B_u}(E) = \sum_n f_n^*(\mathbf{k}^- = \mathbf{0}) f_n(\mathbf{k}^- = \mathbf{0}) \delta(E - E_n). \quad (17)$$

The product of  $I(E)$  and the square of the transition moment will yield the actual spectrum. Using Eqs. (14) and (15), the  $I(E)$ 's are related to the Green's function by the expressions

$$I_{A_u}(E) = \pi^{-1} \text{Im} G_{\mathbf{k}^+ = \mathbf{0}, \mathbf{k}^+ = \mathbf{0}}(E + i\epsilon),$$

$$I_{B_u}(E) = \pi^{-1} \text{Im} G_{\mathbf{k}^- = \mathbf{0}, \mathbf{k}^- = \mathbf{0}}(E + i\epsilon). \quad (18)$$

$I_{A_u}(E)$  and  $I_{B_u}(E)$  will give the "normalized" spectra of mixed crystals polarized along **b** and **ac**, respectively.

The foregoing expressions with the exception of Eqs. (17) and (18) are quite general.  $\{\mathbf{k}\}$  can be any basis set, either localized or delocalized, and  $H'$  can be any

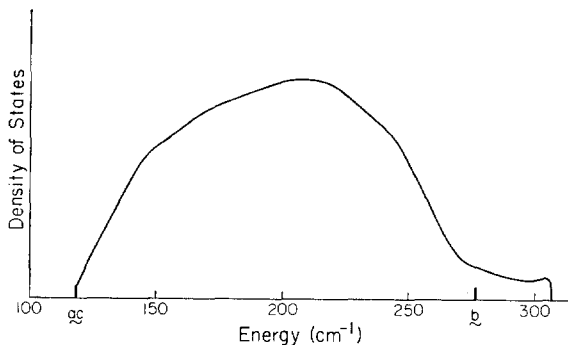


FIG. 6. Density-of-states function obtained experimentally by Colson *et al.*<sup>27</sup> The two Davydov components are represented by two heavy vertical bars.

Hamiltonian, either for a pure or a mixed crystal. Now we are in a position to use the result and to apply it to our problem. We can easily recognize that the secular Eqs. (11a) and (11b) involve nothing but the inverse of the Green's function in a  $\mathbf{k}$  representation. These equations can be rewritten as

$$\sum_{\mathbf{k}'} (E - H')_{\mathbf{k}\mathbf{k}'} f(\mathbf{k}') = 0$$

or

$$\sum_{\mathbf{k}'} G_{\mathbf{k}\mathbf{k}'}^{-1} f(\mathbf{k}') = 0, \quad (19)$$

where

$$G_{\mathbf{k}\mathbf{k}'}^{-1} = (E - E_{\mathbf{k}}) \delta_{\mathbf{k}\mathbf{k}'} - \Delta_{\mathbf{k}\mathbf{k}'},$$

with

$$\Delta_{\mathbf{k}^+ \mathbf{k}'^+} = \Delta_{\mathbf{k}^- \mathbf{k}'^-} = (\Delta/N) [\rho_{\alpha}(\mathbf{k} - \mathbf{k}') + \rho_{\beta}(\mathbf{k} - \mathbf{k}')],$$

$$\Delta_{\mathbf{k}^- \mathbf{k}'^+} = \Delta_{\mathbf{k}^+ \mathbf{k}'^-} = (\Delta/N) [\rho_{\alpha}(\mathbf{k} - \mathbf{k}') - \rho_{\beta}(\mathbf{k} - \mathbf{k}')],$$

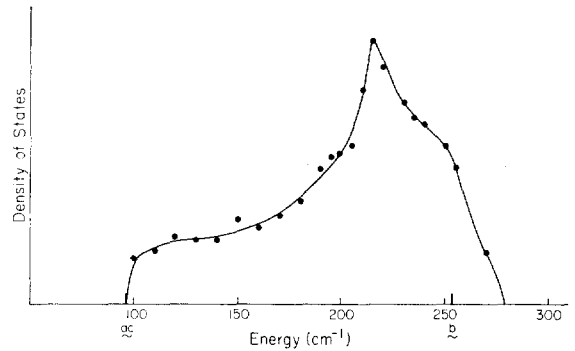


FIG. 7. Density-of-states function according to the octopole model of Craig and Walmsley.<sup>26</sup> The dots indicate the actual values. A smooth curve has been drawn to show the approximate shape of the function.

and the summations are over all  $\mathbf{k}'$  of both exciton branches. Substituting Eq. (9) into Eq. (19), we have

$$G_{\mathbf{k}\mathbf{k}'}^{-1} = [E - \epsilon_A - \epsilon(\mathbf{k})] \delta_{\mathbf{k}\mathbf{k}'} - \Delta_{\mathbf{k}\mathbf{k}'}. \quad (20)$$

We further define

$$G_{\mathbf{k}\mathbf{k}'}^0 = \delta_{\mathbf{k}\mathbf{k}'} / [E - \epsilon_A - \epsilon(\mathbf{k})] = G_0(\mathbf{k}) \delta_{\mathbf{k}\mathbf{k}'}. \quad (21)$$

It can be noted that  $G_0(\mathbf{k})$  is the Green's function for a pure crystal consisting of A only. Such a crystal possesses periodicity, i.e., the quasimomentum  $\hbar\mathbf{k}$  is a good quantum number. Mixing between the  $\mathbf{k}$  states then comes from the perturbation  $\Delta_{\mathbf{k}\mathbf{k}'}$ . Equation (20) can be converted by matrix inversion to yield the Green's function. With the aid of Eq. (21), we find

$$G_{\mathbf{k}\mathbf{k}'} = G_0(\mathbf{k}) \delta_{\mathbf{k}\mathbf{k}'} + G_0(\mathbf{k}) \sum_{\mathbf{k}''} \Delta_{\mathbf{k}\mathbf{k}''} G_{\mathbf{k}''\mathbf{k}'}. \quad (22)$$

This is exactly the matrix form of the operator equation

$$(E - H')^{-1} = (E - H^0)^{-1} + (E - H^0)^{-1} \Delta (E - H')^{-1}.$$

Equation (22) can now be solved by iteration, and we have

$$\begin{aligned} G_{\mathbf{k}\mathbf{k}'} &= G_0(\mathbf{k})\delta_{\mathbf{k}\mathbf{k}'} + (\Delta/N)G_0(\mathbf{k})\rho(\mathbf{k}-\mathbf{k}')G_0(\mathbf{k}') \\ &+ (\Delta/N)^2G_0(\mathbf{k})\sum_{\mathbf{k}''}\rho(\mathbf{k}-\mathbf{k}'')G_0(\mathbf{k}'')\rho(\mathbf{k}''-\mathbf{k}')G_0(\mathbf{k}') \\ &+ (\Delta/N)^3G_0(\mathbf{k})\sum_{\mathbf{k}''}\sum_{\mathbf{k}'''}\rho(\mathbf{k}-\mathbf{k}'')G_0(\mathbf{k}'')\rho(\mathbf{k}''-\mathbf{k}''') \\ &\times G_0(\mathbf{k}''')\rho(\mathbf{k}'''-\mathbf{k}')G_0(\mathbf{k}') + \dots, \quad (23) \end{aligned}$$

where

$$\rho(\mathbf{k}-\mathbf{k}') = \rho_\alpha(\mathbf{k}-\mathbf{k}') + \rho_\beta(\mathbf{k}-\mathbf{k}')$$

or

$$= \rho_\alpha(\mathbf{k}-\mathbf{k}') - \rho_\beta(\mathbf{k}-\mathbf{k}'),$$

depending upon whether  $|\mathbf{k}\rangle, |\mathbf{k}'\rangle$  belong to the same branch or not.

At this point, it is necessary to average over all impurity distributions to obtain an average Green's function. It is exactly this complication that makes the heavily doped mixed crystal much more involved. Similar problems involving the electronic states of a random lattice occupied by two types of atoms have been taken up by Yonezawa and Matsubara.<sup>29a</sup> The corresponding problem for lattice vibrations was also treated by Leath and Goodman<sup>34</sup> using essentially the same formulation. However, only a simple lattice with but one molecule per unit cell was considered in any of these papers. For most organic solids of interest the very existence of multiple exciton branches deserves more careful consideration. In the following section we will proceed with the averaging process to see what complications, if any, arise for the case of multiple exciton branches.

### C. The Average Green's Function

To find the average Green's function, it is necessary to evaluate the  $s$  moments of the  $\rho$ 's defined as

$$M_s(\mathbf{p}_1, \mathbf{p}_2, \mathbf{p}_3, \dots, \mathbf{p}_s) = \langle \rho(\mathbf{p}_1)\rho(\mathbf{p}_2)\rho(\mathbf{p}_3)\dots\rho(\mathbf{p}_s) \rangle_{Av} \quad (24)$$

with

$$\mathbf{p}_1 = \mathbf{k} - \mathbf{k}', \quad \mathbf{p}_2 = \mathbf{k}' - \mathbf{k}'', \quad \mathbf{p}_3 = \mathbf{k}'' - \mathbf{k}''', \text{ etc.}$$

In terms of these moments, the average Green's func-

tion  $\langle G_{\mathbf{k}\mathbf{k}'} \rangle$  is found from Eq. (23) to be

$$\begin{aligned} \langle G_{\mathbf{k}\mathbf{k}'} \rangle &= G_0(\mathbf{k})\delta_{\mathbf{k}\mathbf{k}'} + (\Delta/N)G_0(\mathbf{k})M_1(\mathbf{k}-\mathbf{k}')G_0(\mathbf{k}') \\ &+ (\Delta/N)^2G_0(\mathbf{k})\sum_{\mathbf{k}''}M_2(\mathbf{k}-\mathbf{k}'', \mathbf{k}''-\mathbf{k}')G_0(\mathbf{k}'')G_0(\mathbf{k}') \\ &+ (\Delta/N)^3G_0(\mathbf{k})\sum_{\mathbf{k}''}\sum_{\mathbf{k}'''}M_3(\mathbf{k}-\mathbf{k}'', \mathbf{k}''-\mathbf{k}', \mathbf{k}''-\mathbf{k}''') \\ &\times G_0(\mathbf{k}''')G_0(\mathbf{k}'')G_0(\mathbf{k}') + \dots \quad (25) \end{aligned}$$

The average over all impurity distributions can be effected by replacing the sum over all impurity sites by the sum over all lattice sites multiplied by the impurity concentration:

$$\sum_{\{l\}} \rightarrow C_B \sum_n,$$

where  $\{l\}$  means the average over all possible distributions of  $l$  impurities. In doing this, we must take special care in the cases where impurity sites coincide in the summation of Eq. (24). We will evaluate directly some moments of  $\rho$  to illustrate the general approach to this problem.

For  $s=1$ , two cases can be distinguished:

(I)  $|\mathbf{k}\rangle, |\mathbf{k}'\rangle$  belong to the same exciton branch,

$$M_1(\mathbf{p}_1) = \langle \sum_{l_\alpha} \exp(-i\mathbf{p}_1 \cdot \mathbf{R}_{l_\alpha}) + \sum_{m_\beta} \exp(-i\mathbf{p}_1 \cdot \mathbf{R}_{m_\beta}) \rangle_{Av},$$

where  $l$  impurities occupy  $\alpha$  sites and  $m$  impurities occupy  $\beta$  sites with  $l+m=C_B N$ , the total number of impurities. Replacing the impurity sum by a lattice sum, we have

$$M_1(\mathbf{p}_1) = C_B [ \sum_{n_\alpha} \exp(-i\mathbf{p}_1 \cdot \mathbf{R}_{n_\alpha}) + \sum_{n_\beta} \exp(-i\mathbf{p}_1 \cdot \mathbf{R}_{n_\beta}) ],$$

where  $n_\alpha$  and  $n_\beta$  run over all  $\alpha$  sites and  $\beta$  sites. Therefore,

$$M_1(\mathbf{p}_1) = C_B N \delta(\mathbf{p}_1). \quad (26a)$$

(II)  $|\mathbf{k}\rangle, |\mathbf{k}'\rangle$  belong to different branches,

$$\begin{aligned} M_1(\mathbf{p}_1) &= \langle \sum_{l_\alpha} \exp(-i\mathbf{p}_1 \cdot \mathbf{R}_{l_\alpha}) - \sum_{m_\beta} \exp(-i\mathbf{p}_1 \cdot \mathbf{R}_{m_\beta}) \rangle_{Av} \\ &= C_B [ \sum_{n_\alpha} \exp(-i\mathbf{p}_1 \cdot \mathbf{R}_{n_\alpha}) - \sum_{n_\beta} \exp(-i\mathbf{p}_1 \cdot \mathbf{R}_{n_\beta}) ] \\ &= 0. \end{aligned} \quad (26b)$$

Similarly, for  $s=2$  we have three cases:

(I)  $|\mathbf{k}\rangle, |\mathbf{k}'\rangle$ , and  $|\mathbf{k}''\rangle$  all belong to the same branch,

$$\begin{aligned} M_2(\mathbf{p}_1, \mathbf{p}_2) &= \langle [ \sum_{l_\alpha} \exp(-i\mathbf{p}_1 \cdot \mathbf{R}_{l_\alpha}) + \sum_{m_\beta} \exp(-i\mathbf{p}_1 \cdot \mathbf{R}_{m_\beta}) ] [ \sum_{l_\alpha} \exp(-i\mathbf{p}_2 \cdot \mathbf{R}_{l_\alpha}) + \sum_{m_\beta} \exp(-i\mathbf{p}_2 \cdot \mathbf{R}_{m_\beta}) ] \rangle_{Av} \\ &= \langle \sum_{l_\alpha} \exp[-i(\mathbf{p}_1 + \mathbf{p}_2) \cdot \mathbf{R}_{l_\alpha}] + \sum_{m_\beta} \exp[-i(\mathbf{p}_1 + \mathbf{p}_2) \cdot \mathbf{R}_{m_\beta}] \rangle_{Av} + \langle \sum_{l_\alpha \neq l_{\alpha'}} \sum_{m_\beta} \exp[-i(\mathbf{p}_1 \cdot \mathbf{R}_{l_\alpha} + \mathbf{p}_2 \cdot \mathbf{R}_{l_{\alpha'}})] \\ &+ \sum_{l_\alpha} \sum_{m_\beta} \exp[-i(\mathbf{p}_1 \cdot \mathbf{R}_{l_\alpha} + \mathbf{p}_2 \cdot \mathbf{R}_{m_\beta})] + \sum_{m_\beta \neq m_{\beta'}} \sum_{l_\alpha} \exp[-i(\mathbf{p}_1 \cdot \mathbf{R}_{m_\beta} + \mathbf{p}_2 \cdot \mathbf{R}_{m_{\beta'}})] + \sum_{l_\alpha} \sum_{m_\beta} \exp[-i(\mathbf{p}_1 \cdot \mathbf{R}_{m_\beta} + \mathbf{p}_2 \cdot \mathbf{R}_{l_\alpha})] \rangle_{Av}. \end{aligned}$$

<sup>34</sup> P. L. Leath and B. Goodman, Phys. Rev. 148, 968 (1966).



Replacing the impurity sum by a lattice sum,

$$M_2(\mathbf{p}_1, \mathbf{p}_2) = C_B \left\{ \sum_{n_\alpha} \exp[-i(\mathbf{p}_1 + \mathbf{p}_2) \cdot \mathbf{R}_{n_\alpha}] + \sum_{n_\beta} \exp[-i(\mathbf{p}_1 + \mathbf{p}_2) \cdot \mathbf{R}_{n_\beta}] \right\} \\ + C_B^2 \left\{ \sum_{n_\alpha \neq n_{\alpha'}} \exp[-i(\mathbf{p}_1 \cdot \mathbf{R}_{n_\alpha} + \mathbf{p}_2 \cdot \mathbf{R}_{n_{\alpha'}})] + \sum_{n_\alpha, n_\beta} \exp[-i(\mathbf{p}_1 \cdot \mathbf{R}_{n_\alpha} + \mathbf{p}_2 \cdot \mathbf{R}_{n_\beta})] \right. \\ \left. + \sum_{n_\beta \neq n_{\beta'}} \exp[-i(\mathbf{p}_1 \cdot \mathbf{R}_{n_\beta} + \mathbf{p}_2 \cdot \mathbf{R}_{n_{\beta'}})] + \sum_{n_\beta, n_\alpha} \exp[-i(\mathbf{p}_1 \cdot \mathbf{R}_{n_\beta} + \mathbf{p}_2 \cdot \mathbf{R}_{n_\alpha})] \right\}.$$

Using the equality:

$$\left[ \sum_{n_\alpha} \exp(-i\mathbf{p}_1 \cdot \mathbf{R}_{n_\alpha}) + \sum_{n_\beta} \exp(-i\mathbf{p}_1 \cdot \mathbf{R}_{n_\beta}) \right] \left[ \sum_{n_\alpha} \exp(-i\mathbf{p}_2 \cdot \mathbf{R}_{n_\alpha}) + \sum_{n_\beta} \exp(-i\mathbf{p}_2 \cdot \mathbf{R}_{n_\beta}) \right] \\ = \sum_{n_\alpha} \exp[-i(\mathbf{p}_1 + \mathbf{p}_2) \cdot \mathbf{R}_{n_\alpha}] + \sum_{n_\beta} \exp[-i(\mathbf{p}_1 + \mathbf{p}_2) \cdot \mathbf{R}_{n_\beta}] \\ + \sum_{n_\alpha \neq n_{\alpha'}} \exp[-i(\mathbf{p}_1 \cdot \mathbf{R}_{n_\alpha} + \mathbf{p}_2 \cdot \mathbf{R}_{n_{\alpha'}})] + \sum_{n_\alpha, n_\beta} \exp[-i(\mathbf{p}_1 \cdot \mathbf{R}_{n_\alpha} + \mathbf{p}_2 \cdot \mathbf{R}_{n_\beta})] \\ + \sum_{n_\beta \neq n_{\beta'}} \exp[-i(\mathbf{p}_1 \cdot \mathbf{R}_{n_\beta} + \mathbf{p}_2 \cdot \mathbf{R}_{n_{\beta'}})] + \sum_{n_\beta, n_\alpha} \exp[-i(\mathbf{p}_1 \cdot \mathbf{R}_{n_\beta} + \mathbf{p}_2 \cdot \mathbf{R}_{n_\alpha})],$$

we have

$$M_2(\mathbf{p}_1, \mathbf{p}_2) = C_B N \delta(\mathbf{p}_1 + \mathbf{p}_2) + C_B^2 [N \delta(\mathbf{p}_1) N \delta(\mathbf{p}_2) - N \delta(\mathbf{p}_1 + \mathbf{p}_2)] \\ = C_B^2 N^2 \delta(\mathbf{p}_1) \delta(\mathbf{p}_2) + (C_B - C_B^2) N \delta(\mathbf{p}_1 + \mathbf{p}_2). \quad (27a)$$

(II)  $|\mathbf{k}\rangle, |\mathbf{k}'\rangle$  belong to the same branch and  $|\mathbf{k}''\rangle$  belongs to the other,

$$M_2(\mathbf{p}_1, \mathbf{p}_2) = \langle [\sum_{l_\alpha} \exp(-i\mathbf{p}_1 \cdot \mathbf{R}_{l_\alpha}) + \sum_{m_\beta} \exp(-i\mathbf{p}_1 \cdot \mathbf{R}_{m_\beta})] [\sum_{l_\alpha} \exp(-i\mathbf{p}_2 \cdot \mathbf{R}_{l_\alpha}) - \sum_{m_\beta} \exp(-i\mathbf{p}_2 \cdot \mathbf{R}_{m_\beta})] \rangle_{\Lambda}.$$

Using the same method, we find that

$$M_2(\mathbf{p}_1, \mathbf{p}_2) = 0. \quad (27b)$$

(III)  $|\mathbf{k}\rangle, |\mathbf{k}''\rangle$  belong to the same branch, and  $|\mathbf{k}'\rangle$  belongs to the other,

$$M_2(\mathbf{p}_1, \mathbf{p}_2) = \langle [\sum_{l_\alpha} \exp(-i\mathbf{p}_1 \cdot \mathbf{R}_{l_\alpha}) - \sum_{m_\beta} \exp(-i\mathbf{p}_1 \cdot \mathbf{R}_{m_\beta})] [\sum_{l_\alpha} \exp(-i\mathbf{p}_2 \cdot \mathbf{R}_{l_\alpha}) - \sum_{m_\beta} \exp(-i\mathbf{p}_2 \cdot \mathbf{R}_{m_\beta})] \rangle_{\Lambda} \\ = (C_B - C_B^2) N \delta(\mathbf{p}_1 + \mathbf{p}_2). \quad (27c)$$

It is clear that these expressions can be combined into a single formula if we define the delta function in a broader sense. As an example, take the case of the naphthalene pure crystal where the eigenstates in the  $A_u$  branch can have the same  $\mathbf{k}$  as the eigenstates in the  $B_u$  branch. In the normal sense  $\delta(\mathbf{k} - \mathbf{k}') = 1$  if  $\mathbf{k} = \mathbf{k}'$  no matter whether  $|\mathbf{k}\rangle, |\mathbf{k}'\rangle$  belong to the same branch or not. Using this notation, we will have to treat all possible cases separately as we did above. However, we can define our delta function as

$$\delta(\mathbf{p}_1 + \mathbf{p}_2 + \mathbf{p}_3 + \cdots \mathbf{p}_s) \\ \Rightarrow \delta(\mathbf{p}_1 + \mathbf{p}_2 + \mathbf{p}_3 + \cdots \mathbf{p}_s) H[(-1)^n], \quad (28)$$

where  $H[(-1)^n]$  is the Heaviside step function and  $n$  is the number of  $\mathbf{p}$ 's that connect  $\mathbf{k}$  in one branch and  $\mathbf{k}'$  in the other; so

$$H[(-1)^n] = 0 \quad \text{if } n = \text{odd},$$

$$H[(-1)^n] = 1 \quad \text{if } n = \text{even}.$$

By this definition, we can combine Eqs. (26a), (26b), and (27a)–(27c) to yield a simple expression for  $M_1$

and  $M_2$ ,

$$M_1(\mathbf{p}_1) = C_B N \delta(\mathbf{p}_1), \quad (29a)$$

$$M_2(\mathbf{p}_1, \mathbf{p}_2) = C_B^2 N^2 \delta(\mathbf{p}_1) \delta(\mathbf{p}_2) + (C_B - C_B^2) N \delta(\mathbf{p}_1 + \mathbf{p}_2). \quad (29b)$$

It can be seen that  $M_2$  in Case (II) is equal to zero because  $\delta(\mathbf{p}_2) = 0$ ,  $\delta(\mathbf{p}_1 + \mathbf{p}_2) = 0$ , and  $M_2$  in Case (III) is equal to  $N(C_B - C_B^2) \delta(\mathbf{p}_1 + \mathbf{p}_2)$  because  $\delta(\mathbf{p}_1) = \delta(\mathbf{p}_2) = 0$ .

Formally, Eqs. (29a) and (29b) are analogous to the expressions obtained by YM for the electronic state of binary solids composed of two types of atoms. Physically, we can say that the existence of two branches of exciton states increases the number of intermediate states to which the exciton under scattering can go. Furthermore, in addition to the normal conservation of momentum for the simple case of one molecule per unit cell, the factor-group symmetry must also be retained (*vide infra*). In Fig. 1, we illustrate all these different situations diagrammatically by drawing the possible scattering routes. The correspondence be-

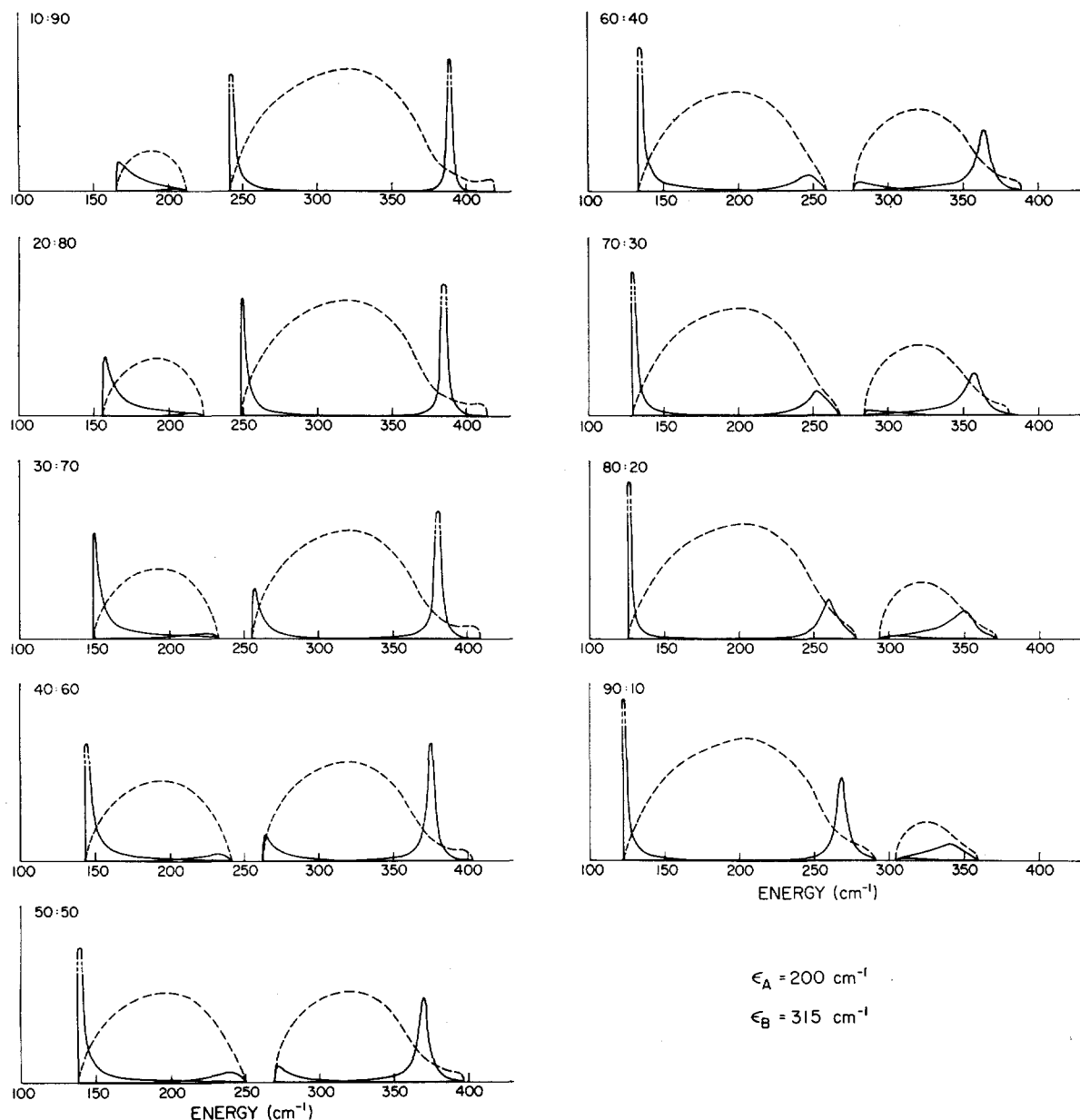


FIG. 8. Calculated density-of-states function (dotted line) and optical spectrum (solid line) for naphthalene- $h_8$  and  $d_8$ , using the experimental density-of-states function of Colson *et al.*<sup>27</sup>  $\epsilon_A$  and  $\epsilon_B$  are band centers for naphthalene- $h_8$  and  $d_8$ , respectively. The concentration ratios given correspond to naphthalene- $h_8$ :naphthalene- $d_8$ .

tween systems with one exciton branch and two exciton branches can be readily seen.

To proceed with the general  $s$  moment, we follow YM<sup>29a</sup> and define a "restricted" lattice average as

$$\langle Y(\mathbf{p}_1) Y(\mathbf{p}_2) Y(\mathbf{p}_3) \cdots Y(\mathbf{p}_s) \rangle_{\Lambda} = \sum_{n_1 \neq n_2 \neq n_3 \cdots \neq n_s} \sum_{t=1}^s (\pm) \exp(-i \sum_{t=1}^s \mathbf{p}_t \cdot \mathbf{R}_{n_t}), \quad (30)$$

where  $n_1 \neq n_2 \neq n_3 \cdots \neq n_s$  means that all  $n_i$ 's are different from one another. Two possible forms of  $Y$ 's are

involved:

$$Y^+(\mathbf{p}) = \sum_{n_\alpha} \exp(-i\mathbf{p} \cdot \mathbf{R}_{n_\alpha}) + \sum_{n_\beta} \exp(-i\mathbf{p} \cdot \mathbf{R}_{n_\beta}),$$

$$Y^-(\mathbf{p}) = \sum_{n_\alpha} \exp(-i\mathbf{p} \cdot \mathbf{R}_{n_\alpha}) - \sum_{n_\beta} \exp(-i\mathbf{p} \cdot \mathbf{R}_{n_\beta}),$$

depending upon whether  $|\mathbf{k}\rangle$ ,  $|\mathbf{k}'\rangle$  belong to the same branch ( $\mathbf{p} = \mathbf{k} - \mathbf{k}'$ ). The signs in front of the exponential depend on whether  $\mathbf{R}_{n_i}$  is  $\mathbf{R}_\alpha$  or  $\mathbf{R}_\beta$ . They also depend on whether  $Y$  is  $Y^+$  or  $Y^-$ .

This definition immediately yields the following

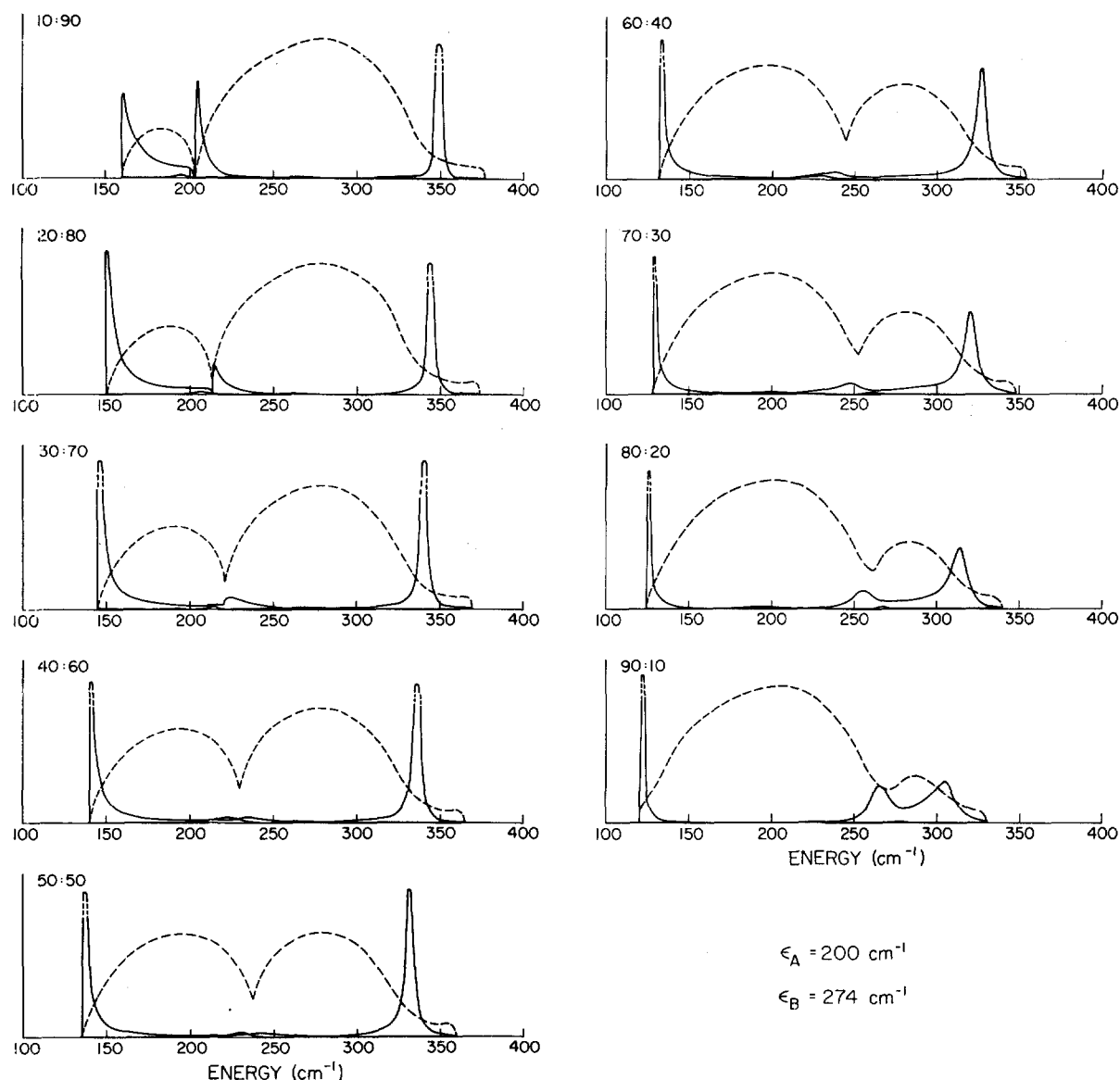


FIG. 9. Calculated density-of-states function and optical spectrum for naphthalene- $h_8$  and naphthalene- $\beta d_4$  using the experimental density-of-states function of Colson *et al.*<sup>27</sup> The conventions are the same as those in Fig. 8.

relation:

$$\exp_L \left[ \sum_j \alpha_j \langle Y(\mathbf{p}_j) \rangle_{Av} \right] = \langle \exp_L \left[ \sum_i \alpha_i Y(\mathbf{p}_i) + \sum_{i \neq j} \sum \alpha_i \alpha_j Y(\mathbf{p}_i + \mathbf{p}_j) + \dots \right] \rangle_{Av}, \quad (31)$$

where  $\exp_L$  is the "leveled exponential" introduced by Kubo,<sup>35</sup>

$$\exp_L \left( \sum_i x_i \right) = 1 + x_1 + x_2 + \dots + x_1 x_2 + x_2 x_3 + \dots + x_1 x_2 x_3 + \dots, \quad (32)$$

with each term containing only the first power of any

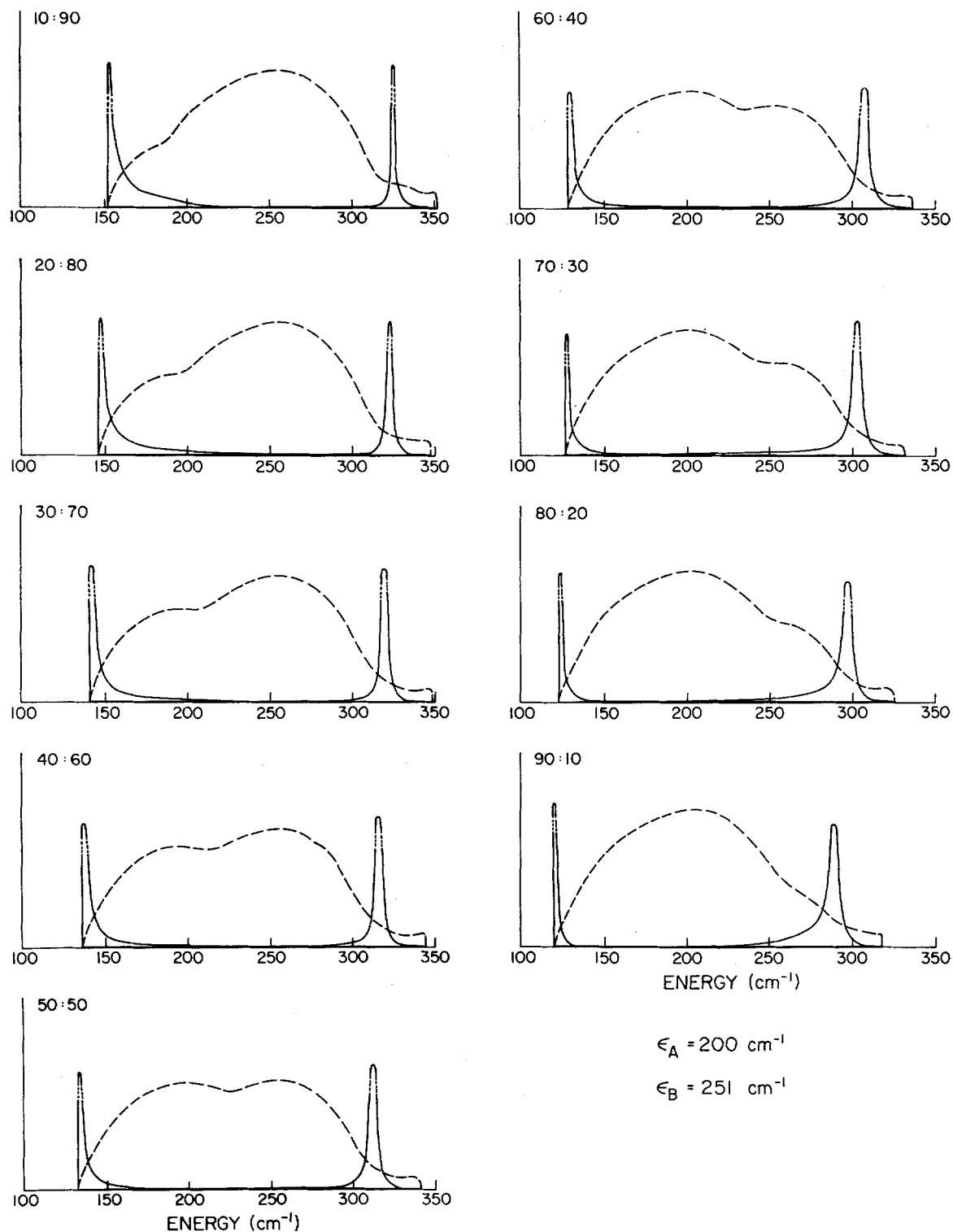
$x_j$ . Equation (31) enables us to express the  $s$  moment of  $Y(s > 1)$  by a sum over various products of the first moment of  $Y$ . The result is

$$\langle Y(p_1) Y(p_2) \dots Y(p_s) \rangle_{Av} = (-1)^s \sum_{\{m\}} \prod_m [-(i_m - 1)!] \times Y_1^m(\mathbf{p}_{1m} + \mathbf{p}_{2m} + \mathbf{p}_{3m} + \dots + \mathbf{p}_{im}), \quad (33)$$

where  $Y_1^m$  is the first moment of  $Y$  with its argument equal to the sum of the  $i_m$   $p$ 's in the  $m$ th compartment of a particular partition.  $\sum_{\{m\}}$  is carried over all the possible partitions  $\{m\}$ . Notice that

$$\sum_m i_m = s.$$

<sup>35</sup> R. Kubo, J. Phys. Soc. Japan 17, 1100 (1962).



Careful examination of the  $Y_1^m$ 's results in the following conclusions:

(i) If there is an even number of  $\mathbf{p}$ 's connecting  $\mathbf{k}$  in one branch and  $\mathbf{k}'$  in the other,

$$Y_1^m = \sum_{n\alpha} \exp[-i(\mathbf{p}_{1m} + \mathbf{p}_{2m} + \mathbf{p}_{3m} + \cdots \mathbf{p}_{im}) \cdot \mathbf{R}_{n\alpha}] \\ + \sum_{n\beta} \exp[-i(\mathbf{p}_{1m} + \mathbf{p}_{2m} + \mathbf{p}_{3m} + \cdots \mathbf{p}_{im}) \cdot \mathbf{R}_{n\beta}] \\ = N\delta(\mathbf{p}_{1m} + \mathbf{p}_{2m} + \mathbf{p}_{3m} + \cdots \mathbf{p}_{im}).$$

(ii) If there is an odd number of  $\mathbf{p}$ 's connecting  $\mathbf{k}$  in one branch and  $\mathbf{k}'$  in the other,

$$Y_1^m = \sum_{n\alpha} \exp[-i(\mathbf{p}_{1m} + \mathbf{p}_{2m} + \mathbf{p}_{3m} + \cdots \mathbf{p}_{im}) \cdot \mathbf{R}_{n\alpha}] \\ - \sum_{n\beta} \exp[-i(\mathbf{p}_{1m} + \mathbf{p}_{2m} + \mathbf{p}_{3m} + \cdots \mathbf{p}_{im}) \cdot \mathbf{R}_{n\beta}] \\ = 0.$$

If we again define the delta function in a broader sense as in Eq. (28), we can use a single formula for all the cases,

$$Y_1^m = N\delta(\mathbf{p}_{1m} + \mathbf{p}_{2m} + \mathbf{p}_{3m} + \cdots \mathbf{p}_{im}). \quad (34)$$

Formally this is again equivalent to the results of YM.<sup>29a</sup>

A comment should be made at this point. Although the present discussions are limited to the case of two molecules per unit cell, with special reference to the naphthalene singlet, the results we have obtained so far can be extended to more complicated systems such as benzene with four molecules per unit cell. The crucial assumption that has to be made is the one we used in Sec. II.A, namely that the exact crystal wavefunctions can be approximated by a simple linear combination of site functions as a result of weak translationally equivalent interactions. It can be noted that the first factor on the right-hand side of Eq. (28) has to do with the translational symmetry of the lattice, while the second factor has to do with the interchange symmetry of the lattice. In the "restricted" Frenkel limit,<sup>30</sup> the basis functions in Eq. (6) are constructed so that they belong to the irreducible representations of *both* the translational group and the interchange group. Equation (28) simply states that a scattering route is allowed if the product of the characters of these irreducible representations (or states involved in the scattering processes), i.e.,  $\Gamma(\mathbf{k})\Gamma^*(\mathbf{k}')\Gamma(\mathbf{k}'')\Gamma^*(\mathbf{k}''')\cdots$  contains the characters of the totally symmetric representations of *both* the translational group (i.e.,  $\mathbf{p} = \mathbf{k} - \mathbf{k}' + \mathbf{k}'' - \mathbf{k}''' \cdots = 0$ ) and the interchange group (i.e.,  $n = \text{even}$ ). This is a general rule and is suitable for all the multiple-branched exciton bands.

For molecular crystals that do have strong translationally equivalent interactions, the assumption that factor-group operations can be applied to all the  $\mathbf{k}$  states is no longer valid. The wavefunctions would be

(for two molecules per unit cell)

$$\Psi_j(\mathbf{k}) = N^{-1/2}[A(\mathbf{k}, j)\Psi_\alpha(\mathbf{k}) + B(\mathbf{k}, j)\Psi_\beta(\mathbf{k})],$$

where the  $j$ 's denote different exciton branches. Although the formulation presented so far would still be applicable, the lattice sum now takes the following form:

$$Y_1^m(\mathbf{p}_{1m} + \mathbf{p}_{2m} + \cdots \mathbf{p}_{im}) \\ = \left\{ \sum_{n\alpha} A(\mathbf{k}, j) A(\mathbf{k}', j') A(\mathbf{k}'', j'') A(\mathbf{k}''', j''') \cdots \right. \\ \times \exp[-i(\mathbf{p}_{1m} + \mathbf{p}_{2m} + \cdots \mathbf{p}_{im}) \cdot \mathbf{R}_{n\alpha}] \\ \left. + \sum_{n\beta} B(\mathbf{k}, j) B(\mathbf{k}', j') B(\mathbf{k}'', j'') B(\mathbf{k}''', j''') \cdots \right. \\ \times \exp[-i(\mathbf{p}_{1m} + \mathbf{p}_{2m} + \cdots \mathbf{p}_{im}) \cdot \mathbf{R}_{n\beta}] \Big\}.$$

No simple expressions can be written. The  $A(\mathbf{k}, j)$ 's and  $B(\mathbf{k}, j)$ 's would have to be evaluated in order to do further calculations. Fortunately, most low-lying states of molecular crystals seem not to fall into such categories.

To relate the moments of  $\rho$  to the moments of  $Y$ , we further define

$$\langle X(\mathbf{p}_1) X(\mathbf{p}_2) X(\mathbf{p}_3) \cdots X(\mathbf{p}_s) \rangle_{Av} \\ = \sum_{l_1 \neq l_2 \neq \cdots \neq l_s} \sum_{i=1}^s (\pm) \exp(-i \sum_{t=1}^s \mathbf{p}_t \cdot \mathbf{R}_{l_t}), \quad (35)$$

where  $\sum_l$  is the sum over all impurity sites and  $l_1 \neq l_2 \neq \cdots \neq l_s$  means that all  $\mathbf{R}_{l_t}$ 's are different.

The relation between the moments of  $X$  and the moments of  $Y$  can be easily established:

$$\langle X(\mathbf{p}_1) X(\mathbf{p}_2) \cdots X(\mathbf{p}_s) \rangle_{Av} \\ = C_B^s \langle Y(\mathbf{p}_1) Y(\mathbf{p}_2) \cdots Y(\mathbf{p}_s) \rangle_{Av}. \quad (36)$$

An expression similar to Eq. (31) now relates the moments of  $\rho$  to the moments of  $X$ :

$$\langle \exp_L[\sum_j \alpha_j \rho(\mathbf{p}_j)] \rangle_{Av} = \langle \exp_L[\sum_j \alpha_j X(\mathbf{p}_j) \\ + \sum_{i \neq j} \alpha_i \alpha_j X(\mathbf{p}_i + \mathbf{p}_j) + \cdots] \rangle_{Av}. \quad (37)$$

Equations (33)–(37) would enable us to evaluate the various moments and the average Green's function. The final expression for the moments can be conveniently given in terms of the cumulants<sup>29a</sup> through the following equations:

$$\langle \exp_L[\sum_j \alpha_j \rho(\mathbf{p}_j)] \rangle_{Av} = \exp_L[\langle \exp_L[\sum_j \alpha_j \rho(\mathbf{p}_j)] - 1 \rangle_c]. \quad (38a)$$

The  $s$  cumulant is, in turn, given as

$$\langle \rho(\mathbf{p}_1) \rho(\mathbf{p}_2) \cdots \rho(\mathbf{p}_s) \rangle_c = P_s(C_B) N \delta(\mathbf{p}_1 + \mathbf{p}_2 + \cdots \mathbf{p}_s), \quad (38b)$$

where  $P_s(C_B)$  is given by a generating function

$$\log[1 - C_B + C_B \exp(x)] = \sum_{s=1}^{\infty} \frac{P_s(C_B) x^s}{s!}; \quad (38c)$$

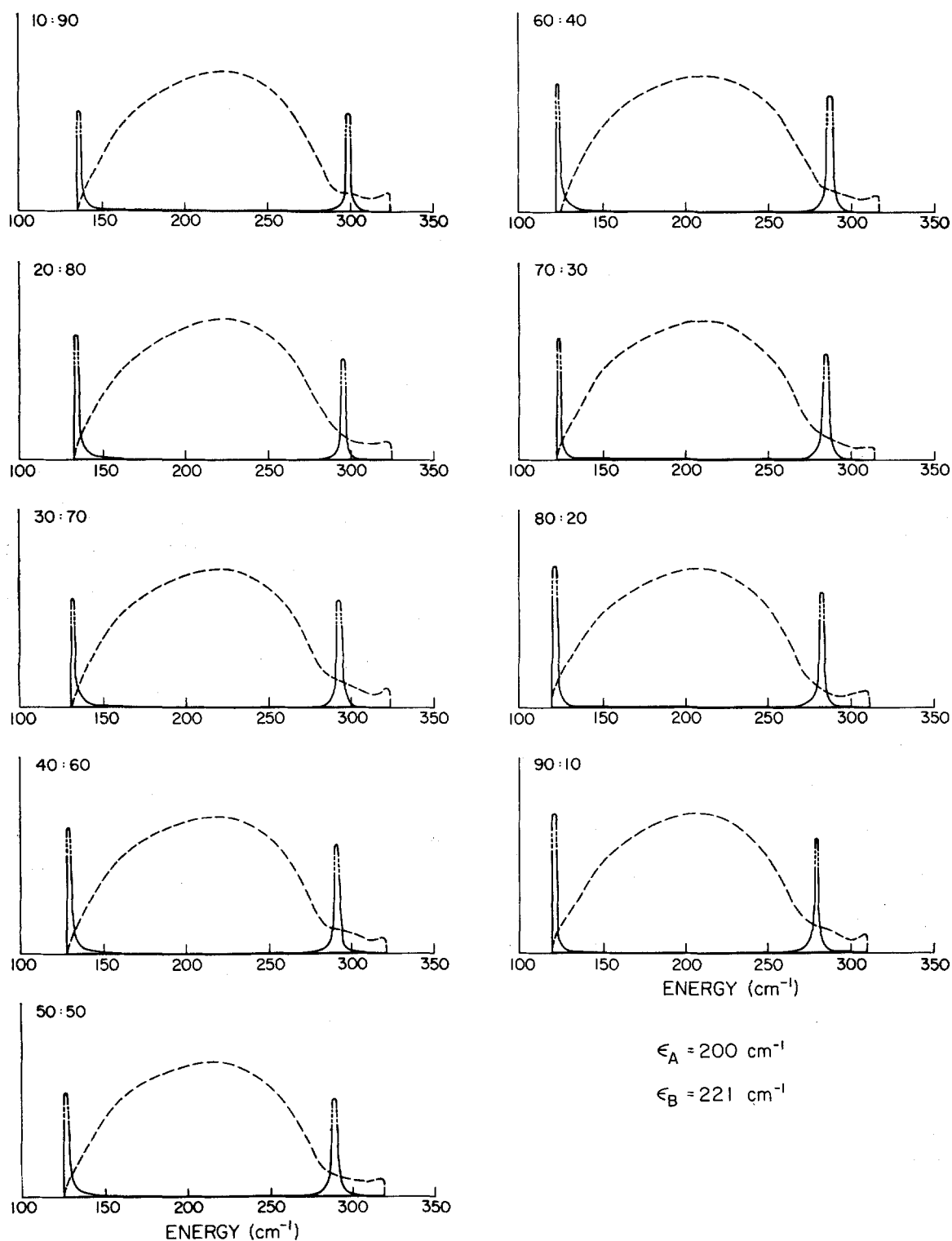


FIG. 11. Calculated density-of-states function and optical spectrum for naphthalene- $h_8$  and naphthalene- $\beta d_1$  using the experimental density-of-states function of Colson *et al.*<sup>27</sup> The conventions are the same as those in Fig. 8.

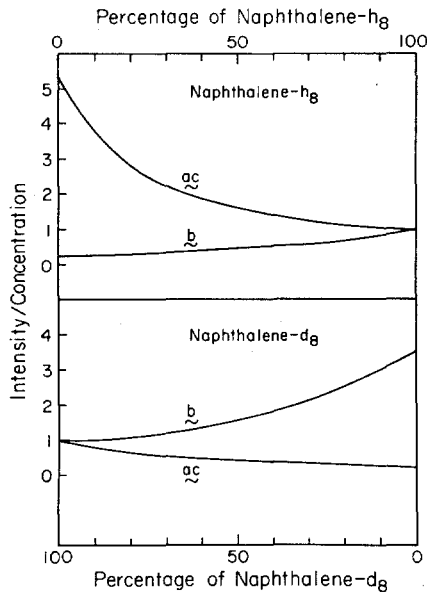


FIG. 12. Intensity distributions of Davydov components for mixed crystals of naphthalene- $h_8$  and  $d_8$  as a function of concentration. Data used here were extracted from Fig. 8 by integrating the optical spectrum.

for example,

$$P_1(C_B) = C_B,$$

$$P_2(C_B) = C_B - C_B^2,$$

$$P_3(C_B) = C_B - 3C_B^2 + 2C_B^3,$$

$$P_4(C_B) = C_B - 7C_B^2 + 12C_B^3 - 6C_B^4, \text{ etc.}$$

The function  $P_s(C_B)$  can be viewed as a probabilistic weighting function and the delta functions contain the "selection rules" of scattering. As shown in the earlier sections, for multiple-branched exciton bands in the "restricted" Frenkel limit, no complications involving the  $P_s$ 's result; however, the delta functions will have to be modified to account for the conservation of factor-group symmetries. Using these equations, the average Green's function is found to be

$$\begin{aligned} \langle G_{kk'} \rangle = & G_0(\mathbf{k})\delta_{kk'} + (\Delta/N)\delta_{kk'}NP_1(C_B)G_0(\mathbf{k})G_0(\mathbf{k}') \\ & + (\Delta/N)^2\delta_{kk'}\{N^2P_1^2(C_B)G_0(\mathbf{k})G_0(\mathbf{k})G_0(\mathbf{k}') \\ & + NP_2(C_B)G_0(\mathbf{k})\sum_{k''}G_0(\mathbf{k}'')G_0(\mathbf{k}')\} \\ & + (\Delta/N)^3\delta_{kk'}\{N^3P_1^3(C_B)G_0(\mathbf{k})G_0(\mathbf{k})G_0(\mathbf{k})G_0(\mathbf{k}') \\ & + N^2P_1(C_B)P_2(C_B)G_0(\mathbf{k})\sum_{k''}G_0(\mathbf{k})G_0(\mathbf{k}'')G_0(\mathbf{k}') \\ & + N^2P_1(C_B)P_2(C_B)G_0(\mathbf{k})\sum_{k''}G_0(\mathbf{k}'')G_0(\mathbf{k}')G_0(\mathbf{k}') \\ & + N^2P_1(C_B)P_2(C_B)G_0(\mathbf{k})\sum_{k''}G_0(\mathbf{k}'')G_0(\mathbf{k}'')G_0(\mathbf{k}') \\ & + NP_3(C_B)G_0(\mathbf{k})\sum_{k''}\sum_{k'''}G_0(\mathbf{k}'')G_0(\mathbf{k}''')G_0(\mathbf{k}')\} \\ & + \dots \quad (39) \end{aligned}$$

Notice that any summation  $\sum_{\mathbf{k}}$  includes all the  $\mathbf{k}$  states in all the branches.

A diagrammatic method in which each expansion term is represented by a diagram drawn in momentum space has been developed by Edwards<sup>36</sup> and Klauder.<sup>37</sup> Equation (39) is depicted diagrammatically in Fig. 2. We have represented the true Green's function by a heavy horizontal line and the free propagator  $G_0$  by a thinner line. Each vertex is associated with a polynomial  $P_s(C_B)$ , where  $s$  equals the number of interaction lines connecting the impurity (represented by a cross) and the exciton line. Each interaction line is associated with a momentum transfer  $\mathbf{p} = \mathbf{k}_1 - \mathbf{k}_2$ , and since the next momentum transfer to a single impurity is zero, each vertex also carries a delta function  $N\delta(\mathbf{p}_1 + \mathbf{p}_2 + \dots + \mathbf{p}_s)$ . The expansion can thus be written down easily by enumerating all the possible diagrams.

These diagrams have the general form of an exciton line with a series of self-energy parts. At this point we define a "proper" self-energy part to be a self-energy part that cannot be split into two parts by cutting the exciton line once. It can be shown that by replacing the last free propagator  $G_0$  with the true propagator  $\langle G \rangle$ , it is now only necessary to sum over all proper self-energy parts. This is demonstrated diagrammatically in Fig. 3. Further simplification can be achieved if all but the first free propagator  $G_0$  in each term is replaced by the true  $\langle G \rangle$ . All the proper self-energy parts that can be broken down into two proper self-energy parts by a closed line cutting through the exciton line twice can be eliminated. This is again shown in Fig. 4. Equation (39) now takes the simpler form

$$\langle G(\mathbf{k}) \rangle = G_0(\mathbf{k}) + G_0(\mathbf{k}) \sum^* (\mathbf{k}) \langle G(\mathbf{k}) \rangle. \quad (40)$$

This is the familiar Dyson equation.<sup>38</sup>  $\sum^* (\mathbf{k})$  denotes the sum of all the irreducible proper self-energy parts and is called the *exciton self-energy*. Alternately, we can rewrite Eq. (40) as

$$\langle G(\mathbf{k}, E) \rangle = 1/[G_0^{-1}(\mathbf{k}, E) - \sum^* (\mathbf{k}, E)]. \quad (41)$$

The argument  $E$  is introduced here to denote the  $E$  dependence.

In order to obtain expressions that are more symmetric with respect to both components, the first constant term in the self-energy can be absorbed into  $G_0^{-1}(\mathbf{k}, E)$ . If we define

$$\Sigma(\mathbf{k}, E) = \sum^* (\mathbf{k}, E) - \Delta C_B,$$

Eq. (41) now becomes

$$\langle G(\mathbf{k}, E) \rangle = 1/[E - C_A \epsilon_A - C_B \epsilon_B - \epsilon(\mathbf{k}) - \Sigma(\mathbf{k}, E)]. \quad (42a)$$

<sup>36</sup> S. F. Edwards, *Phil. Mag.* **3**, 1020 (1958).

<sup>37</sup> R. Klauder, *Ann. Phys. (U.S.)* **14**, 43 (1961).

<sup>38</sup> See, for example, R. D. Mattuck, *A Guide to Feynman Diagrams in Many-Body Problems* (McGraw-Hill Book Co., New York, 1967).

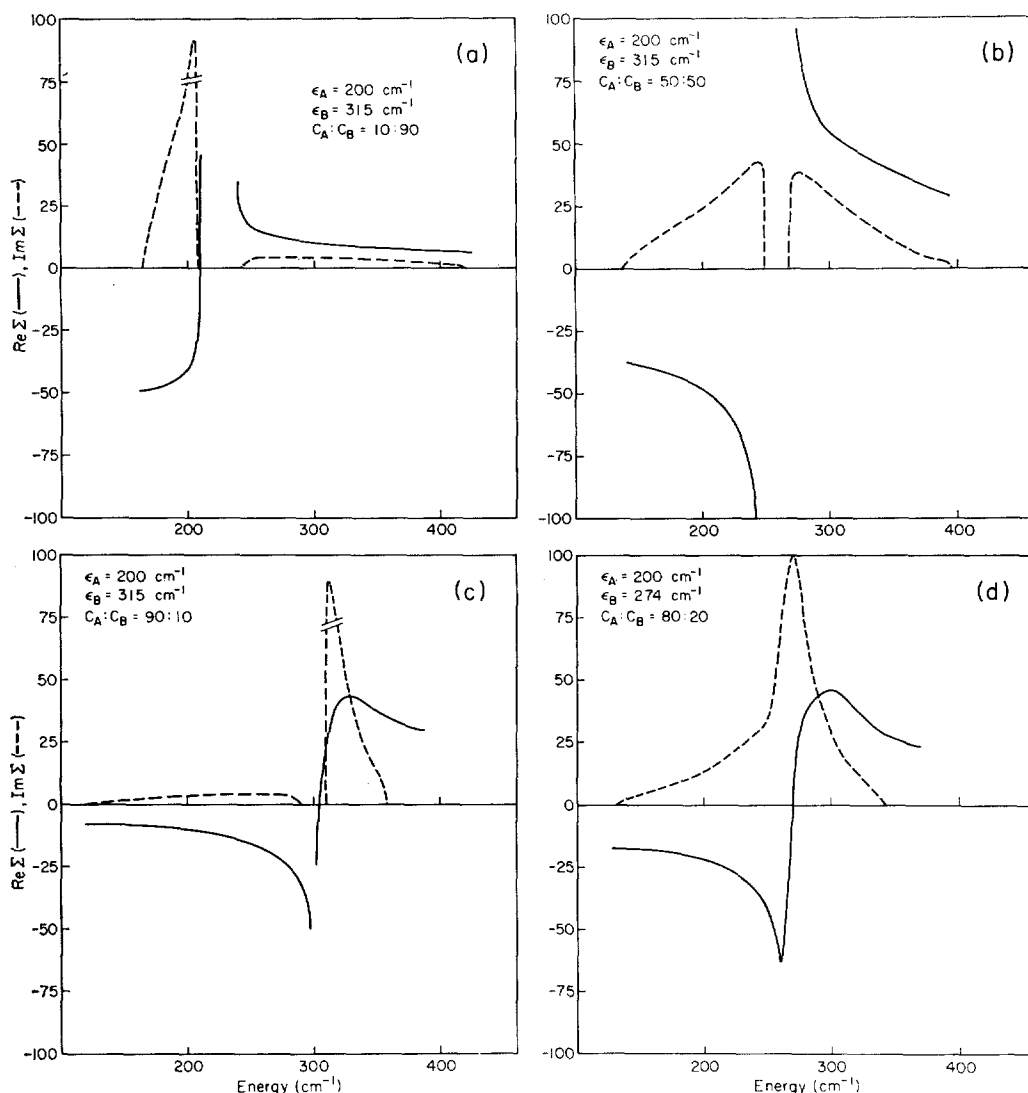


FIG. 13. The behavior of the self-energy  $\Sigma(E)$  calculated from the experimental density-of-states function of Colson *et al.*<sup>27</sup> for (a) 10% naphthalene- $h_8$  and 90% naphthalene- $d_8$ ; (b) 50% naphthalene- $h_8$  and 50% naphthalene- $d_8$ ; (c) 90% naphthalene- $h_8$  and 10% naphthalene- $d_8$ ; and (d) 80% naphthalene- $h_8$  and 20% naphthalene- $\beta d_4$ .

The self-energy, thus defined, can be obtained from Fig. 4 by removing the first diagram from the summation:

$$\begin{aligned}
 \Sigma(\mathbf{k}, E) = & (\Delta/N)^2 NP_2(C_B) \sum_{\mathbf{k}'} \langle G(\mathbf{k}', E) \rangle \\
 & + (\Delta/N)^3 NP_3(C_B) \sum_{\mathbf{k}'} \sum_{\mathbf{k}''} \langle G(\mathbf{k}', E) \rangle \langle G(\mathbf{k}'', E) \rangle \\
 & + (\Delta/N)^4 NP_4(C_B) \sum_{\mathbf{k}'} \sum_{\mathbf{k}''} \sum_{\mathbf{k}'''} \langle G(\mathbf{k}', E) \rangle \\
 & \quad \times \langle G(\mathbf{k}'', E) \rangle \times \langle G(\mathbf{k}''', E) \rangle \\
 & + (\Delta/N)^4 N^2 P_2^2(C_B) \sum_{\mathbf{k}'} \sum_{\mathbf{k}''} \sum_{\mathbf{k}'''} \delta(\mathbf{k} - \mathbf{k}' + \mathbf{k}'' - \mathbf{k}''') \\
 & \quad \times \delta(\mathbf{k}' - \mathbf{k}'' + \mathbf{k}''' - \mathbf{k}) \langle G(\mathbf{k}', E) \rangle \langle G(\mathbf{k}'', E) \rangle \\
 & \quad \times \langle G(\mathbf{k}''', E) \rangle + \dots \quad (42b)
 \end{aligned}$$

We have thus extended YM's results to more complicated systems using a physically reasonable approximation, namely, the neglect of all but short-range forces in the molecular crystal. Equations (42a) and (42b) then become the master equations with which the energy spectrum of mixed crystals can be calculated. It can be seen that the self-energy includes terms that arise from multiple scattering by a single impurity [such as the first, second, and third terms in Eq. (42b)] and also terms that arise from interference scattering by the multiple centers [such as the fourth term in Eq. (42b)]. The former bear no explicit  $\mathbf{k}$  dependence and hence can be calculated if the density-of-states function is known, whereas the latter have to be evaluated from the dispersion relation. A word of caution has to be made about the fourth term and



similar terms associated with two impurities in the expansion. According to our definition of the delta function we draw all the possible scattering routes in Fig. 5. Terms to be included in the sum are those given in Fig. 5(a) and terms to be excluded are those in Fig. 5(b). (We assume  $\mathbf{k}=\mathbf{k}^+$ .) If we define

$$f_1(E, \mathbf{R}) = \sum_{\mathbf{k}^+} \exp(i\mathbf{k}^+ \cdot \mathbf{R}) \langle G(\mathbf{k}^+, E) \rangle \\ + \sum_{\mathbf{k}^-} \exp(i\mathbf{k}^- \cdot \mathbf{R}) \langle G(\mathbf{k}^+, E) \rangle, \\ f_2(E, \mathbf{R}) = \sum_{\mathbf{k}^+} \exp(i\mathbf{k}^+ \cdot \mathbf{R}) \langle G(\mathbf{k}^+, E) \rangle \\ - \sum_{\mathbf{k}^-} \exp(i\mathbf{k}^- \cdot \mathbf{R}) \langle G(\mathbf{k}^+, E) \rangle,$$

we can rewrite the fourth term as

$$(\Delta/N)^4 N^2 P_2^2(C_B) \sum_{\mathbf{k}'} \sum_{\mathbf{k}''} \sum_{\mathbf{k}'''} \delta(\mathbf{k}-\mathbf{k}'+\mathbf{k}''-\mathbf{k}''') \\ \times \delta(\mathbf{k}'-\mathbf{k}''+\mathbf{k}'''-\mathbf{k}) \langle G(\mathbf{k}', E) \rangle \langle G(\mathbf{k}'', E) \rangle \\ \times \langle G(\mathbf{k}''', E) \rangle = (\Delta/N)^4 N^2 P_2^2(C_B) N^{-1} \\ \times \left[ \sum_{\mathbf{R}_e} \exp(i\mathbf{k} \cdot \mathbf{R}_e) f_1(E, \mathbf{R}_e) |f_1(E, \mathbf{R}_e)|^2 \right. \\ \left. + \sum_{\mathbf{R}_i} \exp(i\mathbf{k} \cdot \mathbf{R}_i) f_2(E, \mathbf{R}_i) |f_2(E, \mathbf{R}_i)|^2 \right],$$

where  $\mathbf{R}_e$  is the separation between two translationally equivalent impurities and  $\mathbf{R}_i$  is the separation between two translationally inequivalent impurities. The necessity of using two  $f$  functions to associate with dimers is rather unique for multiple-branch exciton bands. As has been shown in Sec. II.A, energy expressions for translationally equivalent dimers and translationally inequivalent dimers are different. The way we define our delta function will automatically take care of this.

YM<sup>29b</sup> have obtained the second-order self-energy by summing all the diagrams associated with two impurities. They also showed that at low concentrations the second-order self-energy gives the energies of dimers with variable separations consistent with the Koster-Slater equations. A parallel treatment of the present problem would lead to the same conclusion, both the translationally equivalent dimers and inequivalent dimers being obtained in the same limit. Expressions similar to those we have derived in Sec. II.A can be shown to be included in the second-order self-energy.

Although the exact expression of the average Green's function can be written down in an expansion, no closed form has yet been obtained. This is quite expected in view of the fact that we are trying to describe a highly discontinuous function by an analytical expression. In the next section, we will derive an approximation for the average Green's function and apply it to actual numerical calculations.

#### D. Approximate Green's Function and the Calculation of the Naphthalene Mixed-Crystal Energy Spectrum

If we substitute the expressions for the  $P_s$ 's in terms of  $C_A$  and  $C_B$  into Eq. (42b), we have

$$\sum (\mathbf{k}, E) = \Delta^2 C_A C_B [N^{-1} \sum_{\mathbf{k}'} \langle G(\mathbf{k}', E) \rangle] \\ + \Delta^3 C_A C_B (C_A - C_B) [N^{-1} \sum_{\mathbf{k}'} \langle G(\mathbf{k}', E) \rangle]^2 \\ + \Delta^4 C_A C_B (1 - 6C_A C_B) [N^{-1} \sum_{\mathbf{k}'} \langle G(\mathbf{k}', E) \rangle]^3 \\ + [\Delta^4 (C_A C_B)^2 / N^2] \left[ \sum_{\mathbf{k}'} \sum_{\mathbf{k}''} \sum_{\mathbf{k}'''} \delta(\mathbf{k}-\mathbf{k}'+\mathbf{k}''-\mathbf{k}''') \right. \\ \times \delta(\mathbf{k}'-\mathbf{k}''+\mathbf{k}'''-\mathbf{k}) \langle G(\mathbf{k}', E) \rangle \langle G(\mathbf{k}'', E) \rangle \\ \left. \times \langle G(\mathbf{k}''', E) \rangle \right] \\ = \Delta^2 C_A C_B \langle G(E) \rangle [1 - \Delta(C_B - C_A) \\ \times \langle G(E) \rangle + \dots], \quad (43)$$

where

$$\langle G(E) \rangle = N^{-1} \sum_{\mathbf{k}'} \langle G(\mathbf{k}', E) \rangle \\ = N^{-1} \sum_{\mathbf{k}'} [E - C_A \epsilon_A - C_B \epsilon_B - \epsilon(\mathbf{k}') - \sum (\mathbf{k}', E)]^{-1}. \quad (44)$$

This suggests an approximate closed form of the following type:

$$\sum (\mathbf{k}, E) = C_A C_B \Delta^2 / [\langle G(E) \rangle^{-1} + (C_B - C_A) \Delta + \xi]. \quad (45)$$

If we investigate the asymptotic behavior of the self-energy, we find that in the limit of zero bandwidth [ $\epsilon(\mathbf{k})=0$ ], the exact self-energy is given by

$$\sum (E) = C_A C_B \Delta^2 / [E - C_A \epsilon_A - C_B \epsilon_B + (C_B - C_A) \Delta]. \quad (46)$$

To compare Eq. (45) with Eq. (46), we have to assume that the self-energy is  $\mathbf{k}$  independent. Then, when  $\epsilon(\mathbf{k})=0$ ,  $\langle G(E) \rangle^{-1} = E - C_A \epsilon_A - C_B \epsilon_B - \sum (E)$ . It follows immediately that  $\xi = \sum (E)$ . An approximate self-energy is then obtained:

$$\sum (E) = C_A C_B \Delta^2 / [\langle G(E) \rangle^{-1} + (C_B - C_A) \Delta + \sum (E)]. \quad (47a)$$

With this approximate self-energy, Eq. (44) now becomes

$$\langle G(E) \rangle = N^{-1} \sum_{\mathbf{k}'} [E - C_A \epsilon_A - C_B \epsilon_B - \epsilon(\mathbf{k}') - \sum (E)]^{-1}. \quad (47b)$$

Equation (47) has been derived by Taylor<sup>39</sup> for lattice

<sup>39</sup> D. W. Taylor, Phys. Rev. **156**, 1017 (1967).

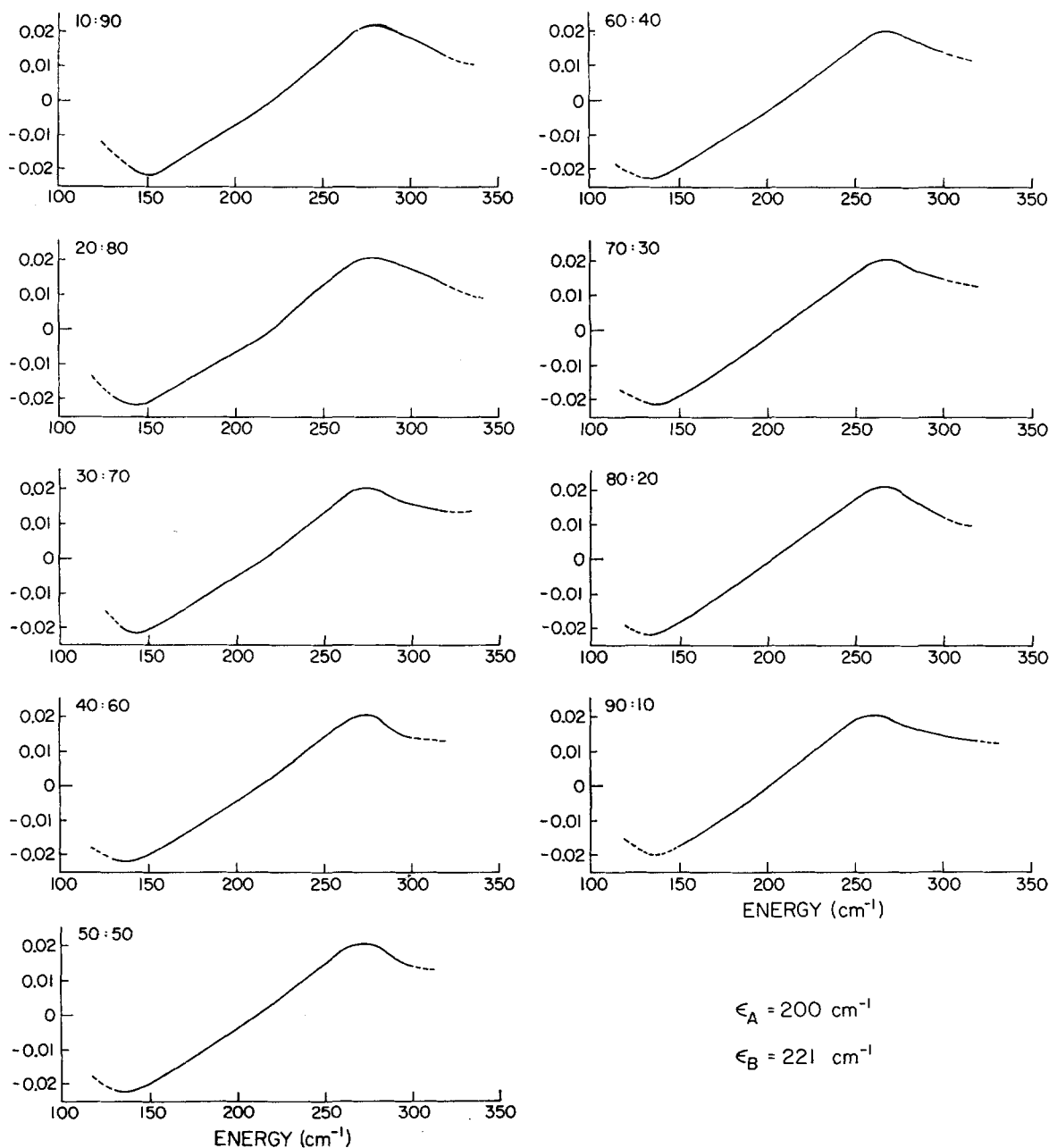


FIG. 14. Calculated  $F$  function (the real part of the Green's function) for mixed crystals of naphthalene- $h_8$  and  $\beta d_1$  using the experimental density-of-states function of Colson *et al.*<sup>27</sup>

vibrations of mixed crystals with mass defects. It was also obtained by Onodera and Toyozawa<sup>40</sup> for the corresponding electron problem. YM<sup>29c</sup> also showed that when the first-order self-energy was expressed as a continued fraction, the lowest approximation agreed with Eq. (47a).

Some features of Eq. (47) can be noted:

(i) It satisfies the dual symmetry, i.e., the equation

is unchanged under the transformation:  $C_A \leftrightarrow C_B$ ,  $\Delta \leftrightarrow -\Delta$ ,  $\epsilon_A \leftrightarrow \epsilon_B$ .

(ii) The mixed-crystal problem can be solved if the density-of-states function is known. The dispersion relation is not needed in this approximation.

(iii) It is exact when  $\epsilon(\mathbf{k}) = 0$  and also when  $\Delta = 0$ .

(iv) It is exact when  $C_B \rightarrow 0$ . In this limit

$$\Sigma(E) = C_B \Delta^2 / [\langle G(E) \rangle^{-1} - \Delta].$$

There is a pole that corresponds to isolated impurities

<sup>40</sup> Y. Onodera and Y. Toyozawa, J. Phys. Soc. Japan 24, 341 (1968).

given by the following relation:

$$N^{-1} \sum_{\mathbf{k}'} [E - \epsilon_A - \epsilon(\mathbf{k}')]^{-1} - (\epsilon_B - \epsilon_A)^{-1} = 0.$$

Our problem now is to solve simultaneously Eqs. (47a) and (47b). Putting  $\langle G(E) \rangle = a + bi$  and  $\sum(E) = c + di$ , we obtain four equations:

$$a = \sum_{E'} \frac{D^0(E') (E - C_A \epsilon_A - C_B \epsilon_B - E' - c)}{(E - C_A \epsilon_A - C_B \epsilon_B - E' - c)^2 + d^2}, \quad (48a)$$

$$b = \sum_{E'} \frac{D^0(E') d}{(E - C_A \epsilon_A - C_B \epsilon_B - E' - c)^2 + d^2}, \quad (48b)$$

$$a = (-cx - dy) / (x^2 + y^2), \quad (48c)$$

$$b = (-dx + cy) / (x^2 + y^2), \quad (48d)$$

where  $D^0(E')$  is the density-of-states function for a pure crystal and

$$x = c[(C_B - C_A)\Delta + c] - d^2 - C_A C_B \Delta^2,$$

$$y = d[(C_B - C_A)\Delta + 2c].$$

Two sets of  $G^0(E')$  are used, one obtained by Craig and Walmsley<sup>26</sup> and the other by Colson *et al.*<sup>27</sup> They are shown in Figs. 6 and 7. Notice that the Davydov components are located  $-77$  and  $81 \text{ cm}^{-1}$  from the mean of the exciton band according to Colson *et al.* and  $-103$  and  $53 \text{ cm}^{-1}$  according to Craig and Walmsley. To solve Eqs. (48), a trial-and-error method was used. A set of trial values for  $c$  and  $d$  was inserted into Eqs. (48) and using Newton's method, a new set of values for  $c$  and  $d$  were obtained. The iterations were carried on until these values converged. Using the results obtained in Sec. II.B, the density-of-states function and the optical spectrum were calculated from the following expressions:

$$D(E) = \pi^{-1} \text{Im} \langle G(E) \rangle = b/\pi,$$

$$I(E) = \pi^{-1} \text{Im} \langle G_{00}(E) \rangle$$

$$= \pi^{-1}$$

$$\times \frac{\text{Im} \sum(E)}{[E - C_A \epsilon_A - C_B \epsilon_B - E_0 - \text{Re} \sum(E)]^2 + [\text{Im} \sum(E)]^2}$$

$$= \pi^{-1} \frac{d}{(E - C_A \epsilon_A - C_B \epsilon_B - E_0 - c)^2 + d^2},$$

where the  $E_0$ 's correspond to the energies of the Davydov components.

We have assumed that the two Davydov components are infinitely sharp. In reality, it is observed that the  $\mathbf{b}$  component is somewhat broad. This has not been taken into account in our calculation.

The exact  $I(E)$ ,  $D(E)$  must satisfy some important sum rules. They are

$$\int_{-\infty}^{\infty} I(E) dE = 1, \quad (49a)$$

$$\int_{-\infty}^{\infty} EI(E) dE = C_A \epsilon_A + C_B \epsilon_B + E_0, \quad (49b)$$

and

$$\int_{-\infty}^{\infty} D(E) dE = 1, \quad (49c)$$

$$\int_{-\infty}^{\infty} ED(E) dE = C_A \epsilon_A + C_B \epsilon_B. \quad (49d)$$

It is easy to show that our approximate  $I(E)$ ,  $D(E)$  also satisfy these sum rules. Equations (49a) and (49b) state that the approximate  $I(E)$  and  $D(E)$  are correctly normalized and Eqs. (49b) and (49d) state that they satisfy the "rule of the lever."

### III. RESULTS AND DISCUSSION

#### A. Calculations Based on Experimental Density-of-States Functions

As we have discussed in Sec. II.D, the mixed-crystal density-of-states function and optical spectrum are completely determined in the first approximation by the over-all density-of-states function (including both exciton branches) and energy gap. The assumption that self-energy does not depend on  $\mathbf{k}$  has the effect of smearing out the density-of-states function that would otherwise be very irregular due to the existence of cluster states.<sup>40</sup> This approximation would suffer severely if the energy gaps were large. For isotopic substitution, the largest possible energy gap is  $115 \text{ cm}^{-1}$ , corresponding to the case of naphthalene- $h_8$  and  $d_8$ . Since the bandwidth is known to be of the same order of magnitude, all the isotopic mixed crystals fall within the limit of shallow traps. The approximation is, therefore, expected to be good.

In Figs. 8–11, we show the results of our calculations for different energy gaps, using the experimental density-of-states function by Colson *et al.*<sup>27</sup> Here the density-of-states function is taken as a 186-point histogram. Each energy interval corresponds to  $1 \text{ cm}^{-1}$ . At fixed energy gap and concentration a particular energy, usually chosen close to  $\epsilon_A$  or  $\epsilon_B$ , is used as a starting point. After the values of  $c$  and  $d$  were calculated from Eqs. (48) by iterations for that energy, they are corrected for energy change and used as the trial values for the next energy interval both higher and lower by  $1 \text{ cm}^{-1}$ . Using this procedure, we can scan the whole region where the density-of-states is nonvanishing. In situations such as naphthalene- $h_8$  in  $d_8$ , two bands exist and two starting points are needed to cover both domains; otherwise one would be sufficient. The convergence is excellent except at band edges. This was also noted by Taylor.<sup>39</sup> However, we did not use his procedure and stopped wherever the density of states was sufficiently small.

In Fig. 8, where the energy gap corresponds to that for  $C_8H_{10}$ – $C_8D_{10}$  mixed crystals, we notice that for all concentrations the eigenstates of the mixed crystal are grouped into two bands. This is due to the moderately

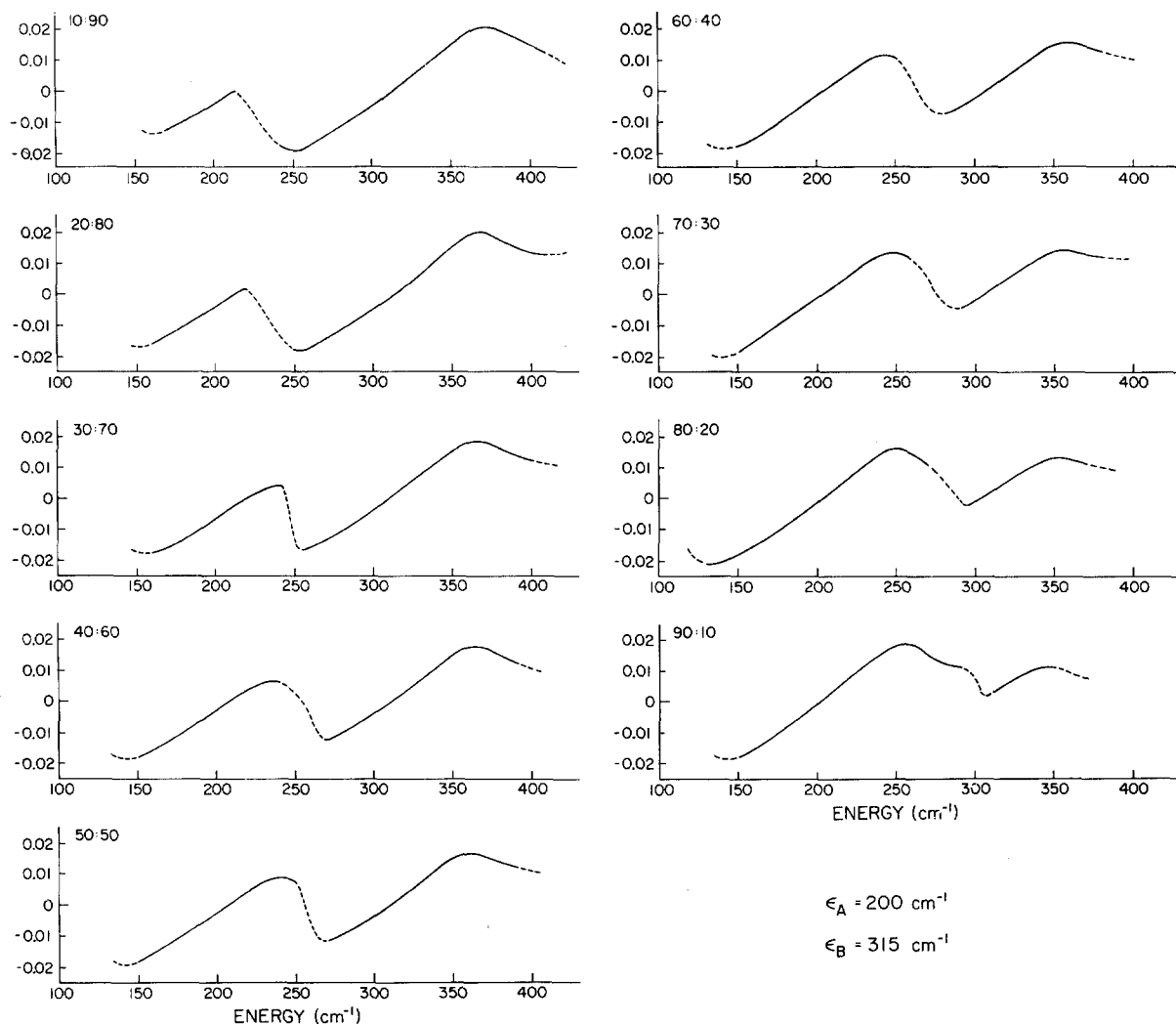


FIG. 15. Calculated  $F$  function (the real part of the Green's function) for mixed crystals of naphthalene- $h_8$  and  $d_8$  using the experimental density-of-states function of Colson *et al.*<sup>27</sup>

large energy gap involved. Each component forms its own exciton band with little disturbance from the other. Davydov splittings similar to those of the pure crystal arise naturally as a result of interactions between like molecules. The density of states attributable to each component is such that the integrated area is equal to the concentration of the component.<sup>39</sup> This is consistent with the fact that the total number of states is not altered by a unitary transformation. Since the shapes of the density-of-states functions in Fig. 8 are all quite similar, the bandwidth increases with concentration, bearing roughly a  $C^{1/2}$  dependence similar to the findings of Onodera and Toyozawa<sup>40</sup> and Taylor.<sup>39</sup> It can also be noted that the mean of the individual exciton bands is shifted relative to the mean energies  $\epsilon_A$  and  $\epsilon_B$  of the pure-crystal exciton bands, indicating the existence of a "repulsive interaction" between the bands. Eventually as  $C \rightarrow 0$ , these interactions will

move the *ideal mixed-crystal level* to the isolated impurity level causing the quasisresonance shift.<sup>8</sup>

Lifshitz<sup>18</sup> has recently given an extensive discussion of the systematics of the energy levels and behavior of band edges in disordered systems. In particular, he predicted that when the perturbation is strong enough to split a state from the main band to form a localized impurity state, the edge of the main band will move to higher energies as more impurities are introduced. This prediction is in agreement with our results.

The Davydov components are seen to be broadened by disordering. For the inner bands, the broadening is much larger due to the proximity of the top of the lower band and the bottom of the upper band. Since the **ac** component is assumed to be at the bottom of the band, it is broadened to only one side, whereas the **b** component, which is inside the band, is seen to be broadened on both sides with more broadening on the

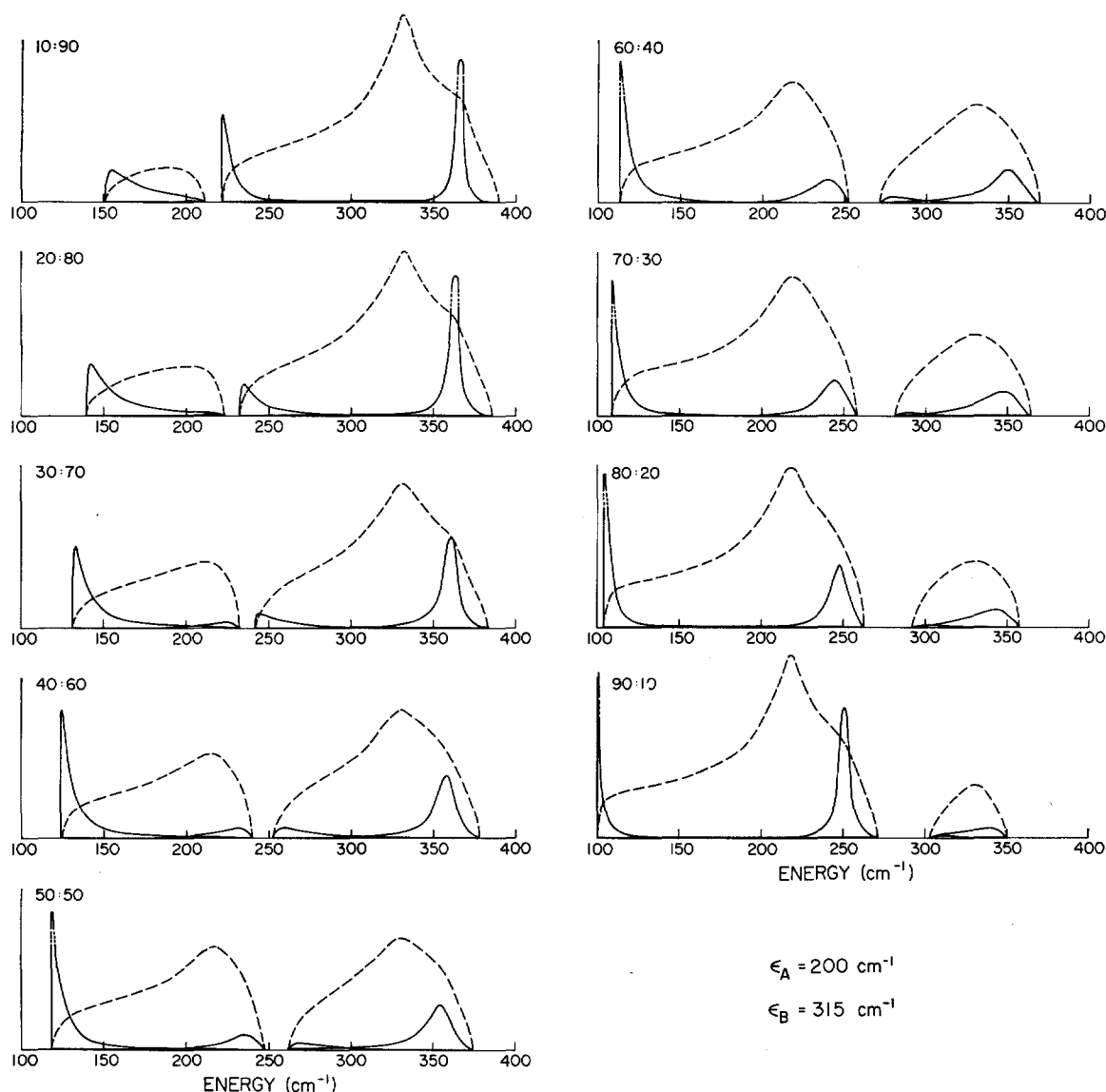


FIG. 16. Calculated density-of-states function (dotted line) and optical spectrum (solid line) for naphthalene- $h_8$  and  $d_8$  using the octopole model. The conventions are the same as those in Fig. 8.

side that has larger density of states. Recently, Sommer and Jortner<sup>16</sup> have suggested looking for the background absorption in the main band induced by isolated impurities as a means of monitoring the band structure. It would appear from Fig. 8 (and the later figures as well) that little can be learned about the over-all band structure by looking at disorder-induced spectra even at high impurity concentrations.

If we turn our attention now to the intensity distribution of the Davydov components, we observe that the outer bands are enhanced and the inner bands weakened. This agrees qualitatively with Sheka's<sup>25</sup> experiment and Broude and Rashba's<sup>23</sup> approximate formula. The integrated absorption intensity attributable to each component divided by its concentration is

plotted in Fig. 12. It can be seen that these values converge nicely to the corresponding values for dilute mixed crystals (as  $C \rightarrow 0$ ) as given by Rashba's<sup>9</sup> equation:

$$I = \left( \frac{1}{E - E(0)} \right)^2 \left( N^{-1} \sum_{\mathbf{k}} \frac{1}{[E - \epsilon(\mathbf{k})]^2} \right)^{-1} \\ = \left( \frac{1}{E - E(0)} \right)^2 \left( \sum_{E'} \frac{D^0(E')}{(E - E')^2} \right)^{-1}.$$

The fact that the outer bands are stronger and sharper indicates that they are relatively undisturbed by the presence of the impurities. This, of course, is due to the large energy difference between the perturbing and the perturbed states. As the bandwidth

increases so does the Davydov splitting until it reaches the limit of full Davydov splitting manifested by the pure crystal. According to the density-of-states function of Colson *et al.*,<sup>27</sup> the Davydov components are located near the bottom and the top of the band. This results in a near- $C^{1/2}$  dependence for the Davydov splittings. Broude and Rashba's allegation that the sum of the Davydov splittings must be equal to the Davydov splitting of the pure crystal is certainly not consistent with the present calculations. In fact, we will show in Part II of this series that our experimental results agree with our calculation rather than with Broude and Rashba's.

Notice that at low concentrations both the theoretical optical spectrum and the density-of-states function are rather structureless. This is probably the most vulnerable region as far as the applicability of the theory is concerned. Experimental data also indicate that although the theory predicts a reasonably good band edge it does not, as expected, show the fine structure observed in the optical spectrum.

Finally, our numerical results indicate that the calculated  $I(E)$  and  $D(E)$  remain correctly renormalized and their first moments equal to  $C_A\epsilon_A + C_B\epsilon_B + E_0$  and  $C_A\epsilon_A + C_B\epsilon_B$ , respectively, within a few wavenumbers. Thus the sum rules in Eqs. (49) are satisfied. This provides a good check on the iteration.

Proceeding now to shallower trap depths, we show in Fig. 9 our calculated results for naphthalene- $h_8$  and  $\beta d_4$ . The energy gap in this case is  $74\text{ cm}^{-1}$ . It can be seen that two bands attributable to naphthalene- $h_8$  and  $\beta d_4$  merge together when the  $h_8$  concentration is larger than 30%, and are barely separated at lower concentrations. The **b**-polarized absorption has a peak in the region  $300\sim 350\text{ cm}^{-1}$ , which is reminiscent of the **b**-polarized absorption of  $\beta d_4$ ; but it also extends throughout the entire band and shows a small hump in the  $h_8$  region, roughly corresponding to the **b**-polarized absorption of  $h_8$ . The **ac**-polarized absorption behaves quite similarly. Compared with the results of  $h_8$  in  $h_8$ , the inner components are here weaker and broader while the outer components are stronger.

If we use Izyumov's<sup>19</sup> method to calculate the isolated impurity states, we find that  $E_r = 180\text{ cm}^{-1}$  for  $h_8$  in  $\beta d_4$  and  $E_r = 291\text{ cm}^{-1}$  for  $\beta d_4$  in  $h_8$ . (The energy reference is the same as in Fig. 9.) The former corresponds to a bound state and the latter to a virtual state. It is interesting to note that, as the concentration of  $h_8$  is lowered to less than 10%, the  $h_8$  band tends to separate from the  $\beta d_4$  band and to form a bound state. On the contrary, when the concentration of  $\beta d_4$  is lower than 10%, the entire  $\beta d_4$  band will be embedded into the  $h_8$  band and produce a virtual state. The last graph in Fig. 9 is quite similar to Fig. 6 of Sommer and Jortner's paper,<sup>16</sup> except that here we are talking about virtual states involving large impurity concentrations. The behavior of the spectrum at lower concentrations of  $\beta d_4$  is such that the peak at  $305$

$\text{cm}^{-1}$  will move to lower energy and converge to  $291\text{ cm}^{-1}$  (a virtual state), and the peak at  $265\text{ cm}^{-1}$  will move to  $277\text{ cm}^{-1}$  (the **b** component of  $h_8$ ). Virtual states are frequently difficult to locate. Our calculation suggests that by following the **b** component of the  $\beta d_4$ , which is relatively strong, and extrapolating to  $C \rightarrow 0$ , we can locate the virtual state. Of course, this depends on the accurate determination of the band position, which may not be so easy for the naphthalene **b** component due to its inherent broadness.

As we proceed to a smaller energy gap, we find that the inner Davydov components almost disappear. For naphthalene- $h_8$  and  $\alpha d_4$  with  $\Delta = 51\text{ cm}^{-1}$ , only two absorption peaks are apparent in Fig. 10. The assignment of each peak to each component has to be made very carefully. We first examine the isolated impurity states. They are found to be  $169\text{ cm}^{-1}$  for  $h_8$  in  $\alpha d_4$  and  $267\text{ cm}^{-1}$  for  $\alpha d_4$  in  $h_8$ . The former is a bound state being only  $1\text{ cm}^{-1}$  from the main band edge; the latter is a virtual state lower in energy than the **b** component of  $h_8$  ( $277\text{ cm}^{-1}$ ). With this in mind, we can start interpreting the first and the last graphs in Fig. 10. In the first graph, the sharp **b**-polarized absorption is almost pure  $\alpha d_4$ , the broad **ac**-polarized absorption indicates complete mixing of the  $\alpha h_4$   $\mathbf{k}=0$  state with the  $h_8$  impurity states. The mixing is so complete that it is no longer legitimate to speak of the excitation of  $\alpha h_4$  or  $h_8$  alone. The same interpretation can be made for the last graph. The sharp **ac** component is almost pure  $h_8$  and the **b** component now becomes a mixture of the  $h_8$   $\mathbf{k}=0$  state and the  $\alpha d_4$  states. In between these extremes, both the **ac** and **b** components show the effect of mixing and broadening. A gradual transition from the excitation of one molecule to the other occurs over the whole concentration range. The widths of the individual components clearly bear out this fact.

Further reduction in the strength of the perturbation results in a situation not very different from that of the pure crystal. In Fig. 11, we see that for naphthalene- $h_8$  and  $\beta d_1$  ( $\Delta = 21\text{ cm}^{-1}$ ), both the density-of-states function and the optical spectrum approach those of the pure crystal. Two sharp lines are predicted. These lines shift gradually from the Davydov components of the pure  $h_8$  to those of pure  $\beta d_1$ . In the limit of the dilute crystal, no bound state or virtual state will be observed.

The various types of behavior of the self-energy  $\Sigma(E)$  are illustrated in Figs. 13(a)–13(d). It can be seen that the imaginary part of  $\Sigma(E)$  is larger in the impurity region and smaller in the main band [Figs. 13(a) and 13(c)]. Since we are effectively calculating the response of the crystal to wave-type excitation, it is not surprising that the damping of the excitation is larger in the impurity band, which is formed by localized excitations, as compared with the damping in the main band. In Fig. 13(d), we notice that when  $\text{Re}\Sigma(E) = 0$ ,  $\text{Im}\Sigma(E)$  has its maximum. This behavior is somewhat common. The same type of resonance peaking was also

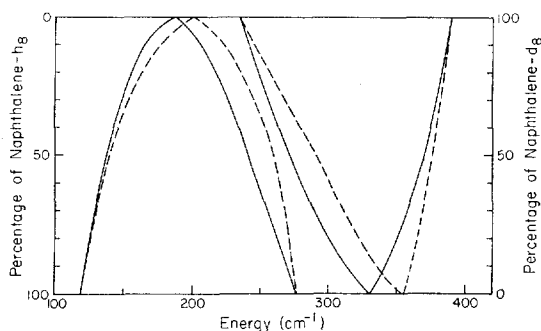


FIG. 17. The calculated absorption maxima of the Davydov components for mixed crystals of naphthalene- $h_8$  and  $d_8$ . Dotted line corresponds to results obtained by using the octopole model, and solid line corresponds to results obtained by using the experimental density-of-states functions. We assumed that the octopole model predicted the correct energies of the Davydov components in the pure crystal; see text.

observed in the similar studies involving lattice vibrations. In fact, Taylor<sup>39</sup> observed the same behavior (see Fig. 3 of his paper) in his calculation of the lattice dynamics of mixed crystals of gold and copper.

The behavior of the real part of the Green's function, which is by definition the principal value of the integral

$$F(E) = P \int [D(E') dE' / (E - E')], \quad (50)$$

is illustrated in Figs. 14 and 15. A useful analogy<sup>19</sup> can be used in the discussion of the general behavior of this function. If  $D(E')$  is understood as the charge distribution function and  $E - E'$  the distance between the point of observation and the charge, the function  $F(E)$  then, by analogy, is the potential function. For a density-of-states function that consists of only one band (Fig. 14), there is only one source. At distances much larger than the dimension of the source, the source can be regarded as a point charge and the potential is inversely proportional to the distance. As the distance is reduced, the potential increases and reaches its maximum near the band edge. On approaching the center of gravity of the distributed charges, the potential decreases due to the mutual compensation of the charges in the outer region and finally equals zero at the center of gravity. Thus the shape of the  $F$  function can be understood in the region  $E >$  the center of gravity. By changing the repulsive potential to the attractive potential we can use the same argument to explain the behavior of the  $F$  function in the region  $E <$  the center of gravity, where the  $F$  function is inverted.

When two bands exist, the behavior of the  $F$  function resembles that of the potential due to two sources. By superimposing two  $F$  functions similar to Fig. 14, we have the situation shown in Fig. 15. The  $F$  function is seen to possess two maxima and two minima due to the presence of two bands.

Notice that the  $F$  functions were not calculated from

Eq. (40), but rather obtained directly as solutions of Eqs. (48). The agreement between the results obtained from Eqs. (50) and (48) is evidence of the self-consistency of Eqs. (48).

## B. Calculations Based on the Octopole Model

Calculations were also performed using the density-of-states function derived from the octopole model of Craig and Walmsley.<sup>26</sup> This was done (1) to study the effect of the density-of-states function of the pure crystal on the density-of-states function and optical spectrum of mixed crystals, and (2) to compare the results obtained by solving Eqs. (48) with those of the incomplete machine calculations by Craig and Philpott.<sup>14</sup> The octopole model of exciton interactions in naphthalene predicts a density-of-states function that is rather asymmetric. As shown in Fig. 16, this asymmetry is carried over to the mixed-crystal density-of-states function. It can be seen that in Fig. 16 the density-of-states functions for 10%  $h_8$ /90%  $d_8$  and 10%  $d_8$ /90%  $h_8$  are quite different. In the former case, the density-of-states function attributable to the guest ( $h_8$ ) is much broader and extends closer to the main band edge, while in the latter case the density-of-states attributable to  $d_8$  is farther from the main band. This is believed to be due to the larger density of states on the higher energy side of the band center and, consequently, larger repulsive interaction felt by the guests when they are above the band. The same effect was also predicted in the theory of impurity levels in dilute crystals. Generalization of this effect to the heavily

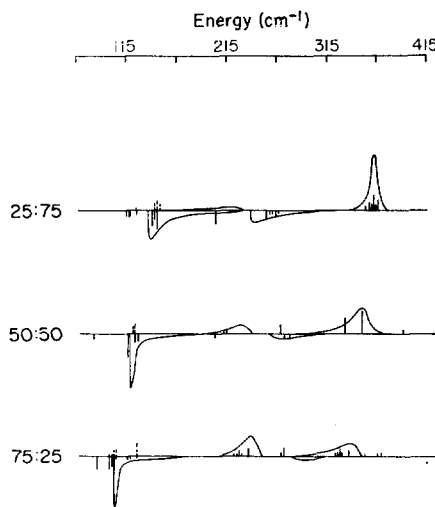


FIG. 18. Comparison between this work (the smooth curves) and the machine calculations by Craig and Philpott<sup>14</sup> (the vertical bars) on the spectra of  $C_{10}H_8$ - $C_{10}D_8$  mixed crystals. The curves (or bars) above the horizontal line represent the b-polarized spectra and those below represent the ac-polarized spectra. The ratios given correspond to naphthalene- $h_8$ :naphthalene- $d_8$ . Intensities are given in arbitrary units.

doped mixed crystals will predict a narrower impurity band for guests above the main band.

To compare with calculations based on the experimental density-of-states function,<sup>27</sup> we have shifted the position of the band center from the octopole model to higher energy so that the two Davydov components coincide with those of Sec. III.A. It should be pointed out that theoretical calculations of the band structure deal only with the intermolecular interactions that lead to the exciton band without any reference to the absolute position of the band center. In principle, the merits of different models for exciton interactions should be weighed by using the band center as the common energy reference. From this point of view, if we accept the absolute position of the band center obtained from hot-band spectroscopy of Colson *et al.*,<sup>27</sup> the octopole model is already erroneous (by 26 cm<sup>-1</sup>) in predicting the absolute positions of the Davydov components, although their relative positions given by the Davydov splitting are in good agreement with experiments. However, since the position of the band center is not directly observable physically, another approach would be to use the position of the lowest Davydov component as common energy reference. In doing this, we are effectively comparing the shape of the density-of-states function in the region spanned by the Davydov components. This approach was adopted by Sommer and Jortner<sup>16</sup> and by Hanson *et al.*<sup>8</sup> and will also be used here.

In Fig. 17, we have plotted the relative positions of the Davydov components of  $h_s/d_s$  mixed crystals as a function of concentration for the two different models. It can be seen that the Davydov components are rather symmetric for the experimental density-of-states function in the sense that the plot has roughly a center of inversion. On the other hand, the octopole model gives a highly asymmetric plot. In the idealized situation where the density-of-states function is symmetric and the Davydov components are located symmetrically with respect to the band center, the plot will have an exact center of inversion. Knowing the Davydov components, we can use this method to gain some information about the shape of the density-of-states function. In this respect, it is an extension of the method of the variation of energy denominators used by Sommer and Jortner<sup>16</sup> and by Hanson *et al.*<sup>8</sup> Both methods were based on the same principle that the optical spectrum is completely determined by the density-of-states function and the energy gap.

The intensity distributions can be discussed by using the "rule of the lever" contained in Eqs. (49). Compared with the calculations based on the experimental density-of-states function, the **ac**-polarized absorption is stronger in the  $h_s$  region and weaker in the  $d_s$  region. The **b**-polarized absorption behaves oppositely. This provides another criterion for comparing the experimental results with different types of density-of-states functions.

Unlike the corresponding lattice problem,<sup>41</sup> complete machine calculations of the electronic levels of heavily doped mixed crystals based on some kind of dispersion relations have been lacking. The only data available for comparison are those of Craig and Philpott.<sup>14</sup> Since their calculations were made for super cells with relatively small dimensions ( $2 \times 2 \times 2$ ), their results can only be regarded as suggestive. In Fig. 18, we compare our calculations with those of Craig and Philpott.<sup>14</sup> The agreement is actually better than expected considering the fact that only a few of all the possible guest distributions were included in their calculation. Notice that we did not compare our results with the "average" energies obtained by Craig and Philpott. Such an averaging process, although intuitively appealing, is not justifiable. What we observe experimentally is not a single level corresponding to the average energy but rather a broad absorption due to all the levels of all the different guest distributions.

As shown in earlier sections, the cluster states that are important when the energy gaps are large and the concentration of one of the components is small are only treated approximately in Eqs. (48). To study the detailed features of the guest band, several approaches are available:

- (1) The present formulation may be improved by including higher-order self-energies. This calculation will become much more involved and may not be feasible for practical purposes.
- (2) Refined machine calculations must be done especially at low guest concentrations. As mentioned by Craig and Philpott,<sup>14</sup> their calculations were very confusing in this region. Some of the features in the guest band cannot be followed with certainty. A more complete calculation would certainly improve the situation.
- (3) Koster and Slater's equations for *isolated* cluster states or its asymptotic form involving larger gaps<sup>42</sup> may be used and extended to higher concentrations by assuming that only broadening occurs. As was pointed out by YM<sup>29</sup> and by Lifschitz,<sup>18</sup> these isolated cluster states formed the low concentration limits of the true cluster states. In the regions where the present calculations fail to show the detailed structure of the guest band, qualitative discussions can be made in terms of these isolated cluster states. This will be discussed more thoroughly in conjunction with our discussions of the experimental results.

<sup>41</sup> A fairly complete machine calculation on the lattice vibrations of disordered solids has been done by D. N. Payton and W. M. Visscher, *Phys. Rev.* **154**, 802 (1967). Similar calculations on the exciton properties of disordered crystals would be very desirable.

<sup>42</sup> At low guest concentrations, these *isolated* cluster states can be observed in a long crystal. See D. M. Hanson, Ph.D. thesis, California Institute of Technology, 1969. Hanson treated the isolated cluster state as a two-body problem, neglecting the interactions with the host band, which is much higher in energy.



### C. Some Comments on Broude and Rashba's Model and Sheka's Experiments

According to Broude and Rashba's<sup>23</sup> simple model, the positions of the optically active levels in a heavily doped mixed crystal are given by the following equation:

$$1/\epsilon_p = \sum_i [C_i/(E - \epsilon_i)], \quad (51)$$

where  $\epsilon_i$  is the "ideal-mixed-crystal" level (or the exciton-band center) of component  $i$  with concentration  $C_i$ , and  $\epsilon_p$  is the energy difference between the Davydov component  $p$  and  $\epsilon_i$ . Using the present notation, we have  $\epsilon_{A_p} = I_{\alpha\alpha}(0) + I_{\alpha\beta}(0)$  and  $\epsilon_{B_p} = I_{\alpha\alpha}(0) - I_{\alpha\beta}(0)$  for naphthalene crystals. Since two Davydov components exist, two equations can be written. For a binary system, each equation is a second-order equation of  $E$ . Two solutions,  $E_{A_p}$ ,  $E_{B_p}$ , will give the excitation energies of A and B, respectively. Thus the theory always predicts four sharp lines in the optical spectrum without taking into account any broadening due to disordering.

Furthermore, the theory also fails to account for the exciton interactions that cause the quasisonance shift in the limit of dilute mixed crystals. According to Eq. (51), when  $C_A$  approaches unity ( $C_B \rightarrow 0$ )  $E_{A_p} = \epsilon_A + \epsilon_p$ , while  $E_{B_p} = \epsilon_B$ . The single-impurity level is predicted to be the same as the "ideal-mixed-crystal" level!

Conceptually, what Broude and Rashba's model really amounts to is a model in which the mixed crystal is considered as a virtual crystal consisting of two non-interacting but interpenetrating crystals of A and B, each possessing perfect lattice symmetry (including both the translational symmetry and the factor-group symmetry). Davydov's formulation for pure crystals is then extended to this type of idealized mixed crystal. The results, thus obtained, are quite expected: a "scaled-down" Davydov splitting due to the increased "lattice" parameter and eventually, at zero concentra-

tion, the ideal-mixed-crystal level without quasisonance shift. In this connection, Craig and Philpott's<sup>14</sup> method is an improvement over Broude and Rashba's in that it takes into account some disordering by allowing random impurity distributions *within* the supercell. However, the translational symmetry among the supercells is, obviously, an artifact. This "residual" symmetry is removed in the present formulation.

Sheka's experiments<sup>24,25</sup> are difficult to assess at this moment because of the uncertainty involved in the determination of the compositions of his samples. We will defer detailed discussion until a later publication of additional experimental results from this laboratory. It is sufficient to mention two of the problems inherent in Sheka's analysis:

(1) The  $\epsilon_i$ 's were determined from Broude's<sup>43</sup> method of vibronic analysis. This method has been criticized by Nieman and Robinson.<sup>2</sup> In this particular case,  $\epsilon_i$  was determined for naphthalene- $h_8$  to be  $\sim 31\,530\text{ cm}^{-1}$ , which is even lower than the isolated impurity level of naphthalene- $h_8$  in  $d_8$  at  $31\,542\text{ cm}^{-1}$ . According to Hanson *et al.*<sup>8</sup> and also Sommer and Jortner,<sup>17</sup> it should be around  $31\,556\text{ cm}^{-1}$ .

(2) To circumvent the difficulties in Broude and Rashba's formula at both  $C_{h_8} \rightarrow 0$  and  $C_{d_8} \rightarrow 0$ , Sheka assumed that  $\epsilon_{h_8}$  and  $\epsilon_{d_8}$  had a linear dependence on the concentrations. Although this modification allowed some superficial consistencies between theory and experiments involving the naphthalene- $h_8$  absorption bands, it also added to the inconsistencies involving the naphthalene- $d_8$  bands.

### ACKNOWLEDGMENT

One of the authors (HKH) would like to thank Dr. David M. Hanson for providing us with the numerical tabulations of the density-of-states functions and for many helpful discussions.

<sup>43</sup> V. L. Broude, Usp. Fiz. Nauk **74**, 577 (1961) [Sov. Phys.—Usp. **4**, 584 (1962)].